Spring 2016

Advancing Methods to Measure the Atmospheric CO2 Sink from Carbonate Rock Weathering

Devon Salley Mr.
Western Kentucky University, devoncs12@gmail.com

ADVANCING METHODS TO MEASURE THE ATMOSPHERIC CO_2 SINK FROM CARBONATE ROCK WEATHERING

A Thesis
Presented to
The Faculty of the Department of Geography and Geology
Western Kentucky University
Bowling Green, KY

In Partial Fulfillment
of the Requirements for the Degree
Master of Science

By
Devon Connor Salley

May 2016

ADVANCING METHODS TO MEASURE THE ATMOSPHERIC CO_2 SINK FROM CARBONATE ROCK WEATHERING

Date Recommended 4/21/16

Dr. Christopher Groves, Director of Thesis

Dr. Michael May

Dr. Fred Siewers

Dr. Jun Yan

4/25/16

Dean, Graduate Studies and Research Date

ACKNOWLDEGMENTS

I would like to thank all the people and organizations that made this research possible. First I would like to thank my advisor, Chris Groves, for constant guidance and encouragement with this project, from start to finish, as well as with other aspects of the graduate school experience, and life in general. I would also like to thank the members of my committee, Dr. Michael May, Dr. Fred Siewers, and Dr. Jun Yan, for their time spent, input, and support throughout this project. I would also like to thank Wendy DeCroix and other faculty or staff members of the Geography and Geology Department who have seemingly always been there to assist in times of need. I would like to thank my family for their support every step of the way with school, as without them I would likely have never even attempted to earn a graduate degree. Finally, this research was made possible by support from the Karst Waters Institute, the Graduate School at Western Kentucky University, the Stan and Kay Sides Environmental Research Scholarship, the Crawford Hydrology Laboratory, Bowling Green Municipal Utilities, Greensburg Water Works, and the United States Geological Survey.

TABLE OF CONTENTS

LIST OF FIGURES

LIST OF TABLES

ADVANCING METHODS TO MEASURE THE ATMOSPHERIC CO_2 SINK FROM CARBONATE ROCK WEATHERING

Devon Connor Salley May 2016 78 Pages

Directed by: Dr. Chris Groves, Dr. Michael May, Dr. Fred Siewers, and Dr. Jun Yan

Department of Geography and Geology Western Kentucky University

With rising atmospheric CO2 concentrations, a detailed understanding of processes that impact atmospheric CO2 fluxes is required. While a sink of atmospheric carbon from the continents to the ocean from carbonate mineral weathering is, to some degree, offset by carbonate mineral precipitation in the oceans, efforts are underway to make direct measurements of these fluxes. Measurement of the continental sink has two parts: 1) measurement of the dissolved inorganic carbon (DIC) flux leaving a river basin, and 2) partitioning the inorganic carbon flux between the amount removed from the atmosphere and the portion from the bedrock. This study attempted to improve methods to measure the DIC flux using existing data to estimate the DIC flux from carbonate weathering within the limestone karst region of south central Kentucky. The DIC flux from the Barren River drainage basin upstream from Bowling Green in southern Kentucky and northern Tennessee, and the upper Green River drainage basin, upstream from Greensburg, Kentucky, was measured, each for a year, using U.S.G.S. discharge data and water-chemistry data from municipal water plants. A value of the (DIC) flux, normalized by time and area of carbonate rock, of 4.29 g km-3 day-1 was obtained for the Barren River, and 4.95 kg km-3 for the Green. These compared favorably with data obtained by Osterhoudt (2014) from two nested basins in the upper Green River with values of 5.66 kg km-3 day-1 and 5.82 kg km-3 day-1 upstream from Greensburg and Munfordville, respectively. Additional normalization of the values obtained in this study

by average precipitation minus evapotranspiration over the area of carbonate rock, or water available for carbonate dissolution, resulted in values of 5.61x107 g C (km3 H20)-1 day-1 (grams of carbon per cubic kilometer of water, per day) for the Barren, and 7.43x107g C (km3 H20)-1 day-1 for the Green River. Furthermore, a statistical relationship between the total DIC flux and time-volume of water available for dissolution has been observed, yielding an r2 value of 0.9478. This relationship indicates that the primary variables affecting DIC flux for these drainage basins are time and the volume of water available for dissolution.

Chapter 1: Introduction

In recent decades, widespread scientific acceptance that human activities are altering rates of global climate change has resulted in a need for a greater understanding of the magnitudes and processes that govern it. Atmospheric carbon dioxide (CO_2) is an important factor that affects current global climate change, as it has throughout geologic history. As a result of human activity, atmospheric CO_2 has now reached levels that exceed natural levels observed from ice core records (Falkowski et al., 2000). Moreover, atmospheric CO_2 levels (Hoffert et al., 1998) and global mean temperature (Cox et al., 2000) are both expected to continue to increase over the next century. This has led to the need for a better understanding of the processes that govern atmospheric CO_2 fluxes in order to predict them accurately and, potentially, to mitigate future changes (Fan et al., 1998; Cox et al., 2000; Falkowski et al., 2000). A prominent area of research is the budgeting of atmospheric CO_2 through identification and quantification of atmospheric carbon sinks and sources. These types of investigations have highlighted the existence of a "missing carbon sink." The known anthropogenic output of CO_2 to the atmosphere minus the uptake of atmospheric CO_2 by known atmospheric CO_2 sink processes is substantially less than the known amount of CO_2 that remains in the atmosphere and, therefore, current atmospheric carbon cycle budgets are unacceptably imprecise (Tans et al., 1990; Sarmiento and Sundquist, 1992; Siegenthaler and Sarmiento, 1993; Sundquist, 1993).

The existence of a "missing sink" of atmospheric CO_2 has resulted in attempts to account more accurately for a terrestrial sink of atmospheric CO_2, including that associated with the weathering of carbonate rocks (*e.g.*, Amiotte Suchet and Probst, 1995;

Liu and Zhao, 2000; Groves and Meiman, 2001; Liu et al. 2008; 2010; 2011). Studies investigating the atmospheric CO_2 sink from carbonate rock weathering have generally been at global scales, using modeling and/or assumed global dissolution rates, or at small/regional scales, generally using limestone rock tablets or high-resolution water chemistry and discharge data. Estimates of the global carbon sink from carbonate rock dissolution range from 0.088 Pg C/a (petagrams (10^{15} g) of carbon per year) (Hartmann et al., 2009) to .608 Pg C/a (Yuan, 1997). The extensive range of these estimates implies that the magnitude of this sink on a global scale is poorly characterized.

Measurement of the CO_2 sink on the continents from carbonate mineral weathering involves two parts: 1) measurement of the inorganic carbon flux leaving a river basin over a given period of time, and 2) partitioning that carbon between the portion removed from the atmosphere and that coming from the carbonate bedrock. While previous investigations have attempted to account for a terrestrial sink of atmospheric CO_2 by weathering of carbonate rocks (e.g., Liu and Zhao 2000; He et al. 2013), this sink is still poorly characterized. The purpose of this research is to improve methods for measuring the inorganic carbon flux from carbonate rock weathering at the river-basin scale, so that this carbon sink effect potentially could be characterized more accurately on a global scale.

This study made use of one year of existing, publically available water-chemistry and discharge data for two river basins, along with geologic, hydrologic, local precipitation, and temperature data. The total dissolved inorganic carbon (DIC) flux was measured over a year for the Barren River upstream from Bowling Green (October 1, 2012-September 30, 2013) and the Green River upstream from Greensburg (February 1,

2013-January 31, 2014), and then normalized by time, water availability for carbonate rock weathering (precipitation minus evapotranspiration (P-ET)), and the extent of carbonate rock outcrops over each area. The following research questions were addressed as a result of this study:

1. Can the inorganic carbon flux associated with carbonate mineral weathering in the Barren River basin be quantified using existing, publically available discharge and hydrochemical data?
2. What is the volume of the inorganic carbon flux from carbonate mineral weathering for the Barren River drainage basin upstream from Bowling Green, KY, normalized by time, area of carbonate rock, and precipitation minus evapotranspiration, based on existing data?
3. Does comparison of this normalized value with those measured by Osterhoudt (2014) suggest that this normalization process captures sufficient precision of the flux values so that this method can be expanded over large regions?

Chapter 2: Literature Review

2.1 Introduction

Climate change has become an important topic of public and political conversation and scientific investigation over recent decades. Atmospheric carbon dioxide (CO_2) is an important factor that impacts current global climate change, as it has throughout geologic history. Anthropogenic effects on atmospheric CO_2 concentration resulting from the burning of fossil fuels and deforestation, among other reasons, have led the current atmospheric CO_2 concentration to exceed natural levels observed from ice core records (Falkowski et al., 2000) (Figures 1 and 2). Considering this deviation from natural levels, the scientific community has called for a better understanding of the myriad processes that affect the carbon cycle and the interactions between the carbon cycle and other components of the environment (Sarmiento and Sundquist, 1992; Siegenthaler and Sarmiento, 1993; Sundquist, 1993; Fan et al., 1998; Cox et al., 2000; Falkowski et al., 2000). Among research regarding the carbon cycle, one area of particular interest has been the identification and quantification of atmospheric carbon sources and sinks. A more detailed understanding of the specific sinks and sources of carbon and, therefore, more detailed and accurate carbon budgeting, is critical to make better predictions regarding future atmospheric CO_2 levels and to determine what should be done to ameliorate the increase of atmospheric CO_2 levels.

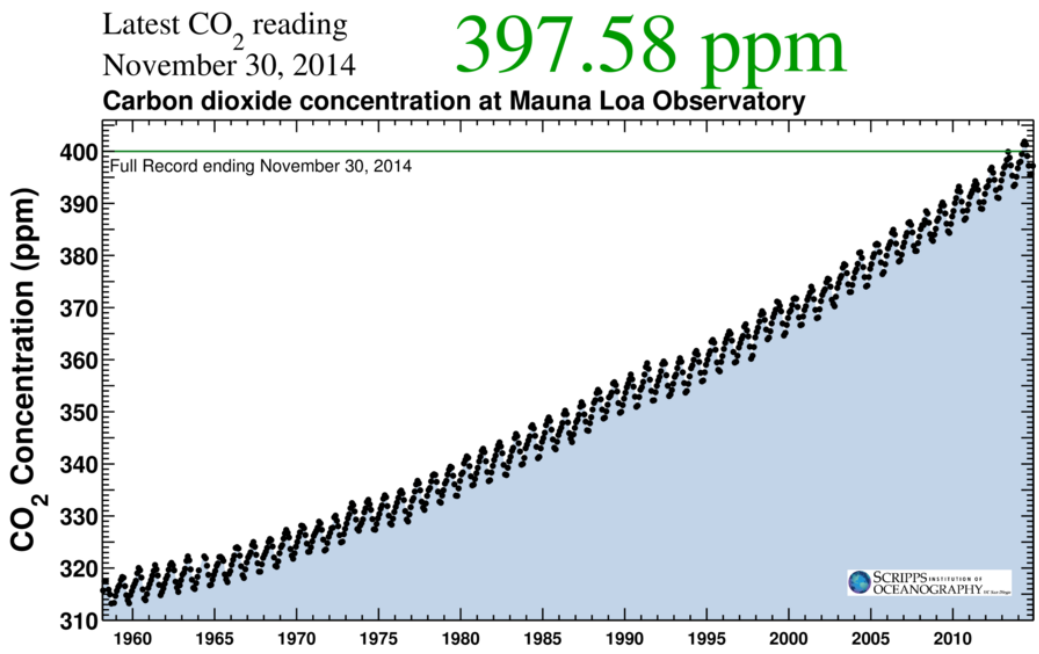

Figure 1: Atmospheric CO_2 concentration since 1958. Source: Tans and Keeling (2014).

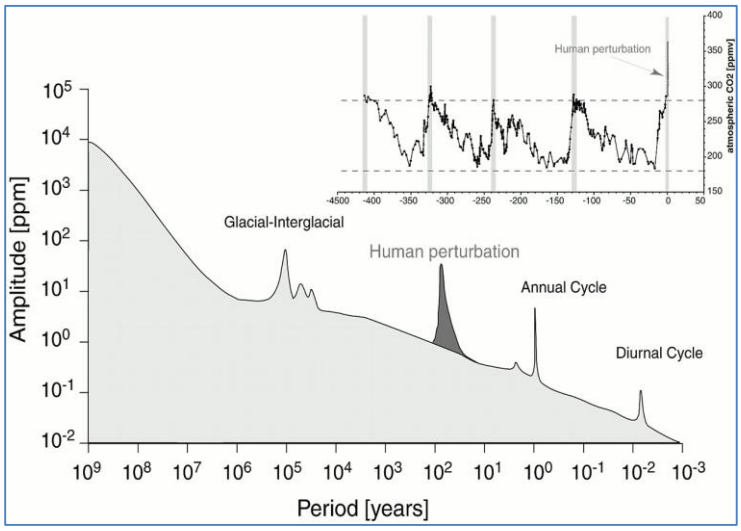

Figure 2: Atmospheric CO_2 concentration over the past 420,000 years. Source: Falkowski et al. (2000).

2.2 The Carbon Cycle and Climate Change

The carbon cycle can be described as the global circulation of carbon through the interactions between the various carbon reservoirs; the exchange of carbon from one reservoir to another is referred to as a carbon flux. Many fluxes into or out of the

atmosphere can be considered as either a net sink of atmospheric carbon, which removes carbon from the atmosphere, or a net source of carbon, which adds carbon to the atmosphere. The primary reservoirs involved in the carbon cycle are (in descending order of magnitude): the earth's crust (Sundquist, 1993) within which the majority of carbon is stored in carbonate rocks (Liu and Zhao, 2000), the intermediate and deep ocean, terrestrial soils and detritus, the surface ocean, the atmosphere, and land biota (Siegenthaler and Sarmiento, 1993; Sundquist, 1993) (Figure 3). It should be noted that Sundquist (1993) described the earth's crust as the largest carbon reservoir, while Siegenthaler and Sarmiento (1993) did not give a direct indication of carbon stored in carbonate rocks or in the earth's crust in their reservoir descriptions. While dividing the carbon cycle into these particular reservoirs is a generalization, as each subdivision has numerous components and, therefore, processes acting upon it, describing them in this way allows for a general understanding of the primary locations of carbon storage and their respective magnitudes.

Past changes in atmospheric CO_2 concentration and associated changes in climate have been the topic of extensive investigation, primarily through the interpretation of ice-core data and, to a somewhat lesser degree, the marine sediment record. A significant controlling factor on climate change through time has been the effect of natural changes in the earth's orbital parameters (Shackleton, 2000; Sigman and Boyle, 2000), known as the Milankovitch (1941) cycles. These orbital parameters include eccentricity, obliquity, and precession occurring in cycles of roughly 100,000 years (100 ky), 41 ky, and 23ky, respectively. Although these cycles play an important role, as they affect the amount of solar radiation received by the Earth, it has been demonstrated that changes in the carbon

cycle and resulting changes in atmospheric CO_2 are also a crucial component of past climate change (Sundquist, 1993; Shackleton, 2000; Sigman and Boyle, 2000). It is known that current atmospheric CO_2 concentrations (see Figures 1, 2, and 3) are higher than any previously recorded within the constraints of the ice record, with natural pre-industrial atmospheric CO_2 concentration fluctuating between 172-300 parts per million by volume (ppmv) (Lüthi et al., 2008), compared to modern concentrations that have now reached levels of 396 ppmv (Tans and Keeling, 2014) (Figure 1). While there is little doubt that human activity has resulted in a change from natural, preindustrial conditions, there is some debate regarding whether or not atmospheric CO_2 was in a steady state before anthropogenic alteration.

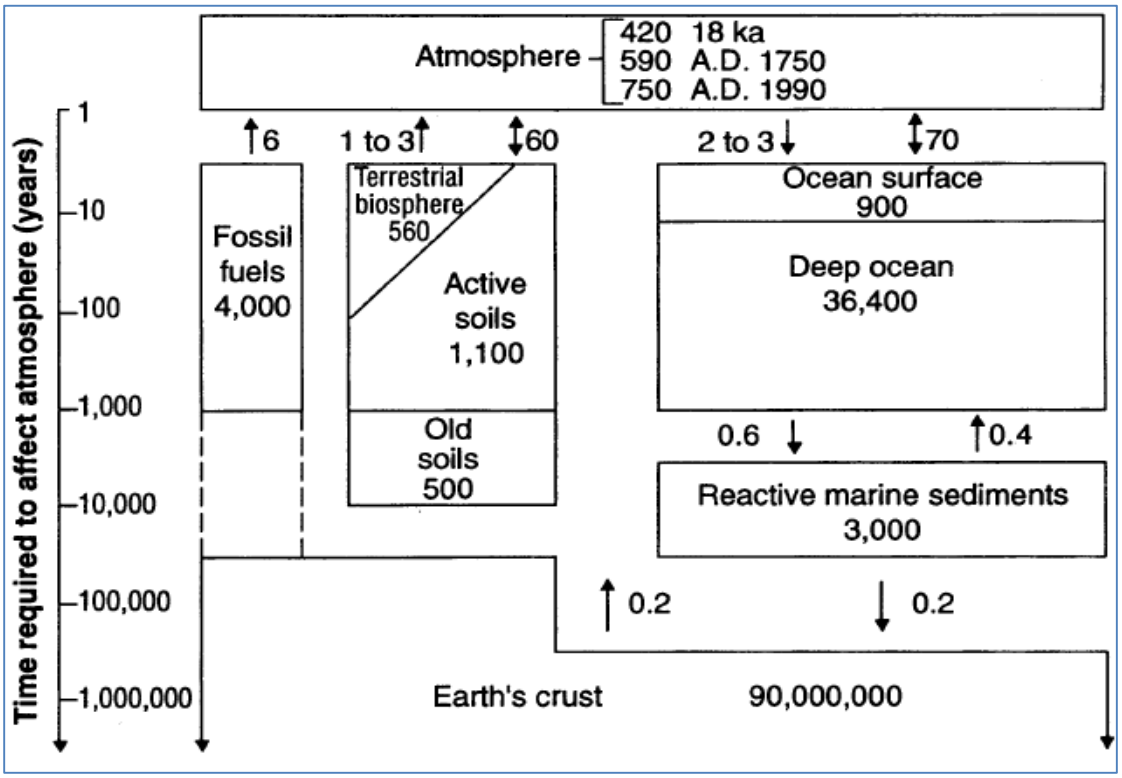

Figure 3: Diagram showing various reservoirs of the carbon cycle. Source: Sundquist (1993).

For example, from their analysis of ice-core data, Lüthi et al. (2008) proposed that there could be significant long-term fluctuations of atmospheric CO_2 concentrations on time scales of 100ky. Additionally, Sundquist (1993) argued that, because of long-term response times to deglaciation of many carbon cycle processes, such as deep-sea calcite ($CaCO_3$) dissolution and soil and sediment carbon accumulation, estimates of CO_2 sinks/sources should be consistent with models that integrate the potential for these effects on the pre-industrial state of the carbon cycle. Conversely, Siegenthaler and Sarmiento (1993), in their global atmospheric CO_2 model, assumed that natural CO_2 variations are relatively small, and that the natural cycle operates in a steady state. Finally, the carbon cycle feedback-coupled climate model of Cox et al. (2000) suggests a pre-industrial steady state between land-atmosphere and ocean-atmosphere carbon fluxes, as well as atmospheric CO_2 concentrations over the long-term average. They also show that estimates of carbon storage in various reservoirs by their model are consistent with other contemporary carbon storage estimates.

This perturbation from the natural cycle discussed above is primarily attributed to the combustion of fossil fuels and widespread deforestation, although the former has had a significantly smaller effect than the latter. Furthermore, it is estimated that, while continued combustion of fossil fuels can still raise future atmospheric CO_2 over current levels by several fold, the continued effect of deforestation is relatively limited (Siegenthaler and Sarmiento, 1993). CO_2 is a "greenhouse gas", that is, it absorbs short-wave energy from sunlight and releases this energy as heat to its surroundings; because of this, increased atmospheric CO_2 has been identified as a primary contributor to global climate change and, more specifically to global atmospheric warming trends or "global

warming." Atmospheric CO_2 has been correlated with atmospheric temperature over the last 400,000+ years from ice core data and, while there have been sharp changes of temperature without CO_2 changes, it seems that a substantial change in CO_2 without a change in temperature has not occurred (Falkowski et al., 2000). Moreover, under currently probable scenarios, atmospheric CO_2 concentrations are destined to increase throughout this century (Hoffert et al., 1998). As a result, using current climate models that integrate feedback effects of climate-carbon cycle interactions, it has been estimated that the global mean temperature may increase by 5.5°C over the coming century (Cox et al., 2000). Given the importance of atmospheric CO_2 with regard to current global climate changes, and likely changes to come, a more complete understanding of the processes that govern atmospheric CO_2 release and uptake, and their magnitude, is needed in order to predict future changes accurately (Sarmiento and Sundquist, 1992; Sundquist, 1993; Fan et al., 1998; Cox et al., 2000; Falkowski et al., 2000).

2.3 Carbon Budgeting and the "Missing Carbon Sink"

Scientific studies regarding atmospheric CO_2 and the carbon cycle have become more frequent, especially over recent decades (Sarmiento and Sundquist, 1992; Sundquist, 1993; Fan et al., 1998; Cox et al., 2000; Einsele et al. 2001; Liu et al. 2008). In these studies, a significant area of investigation has been related to the budgeting of atmospheric CO_2 through identification and quantification of atmospheric carbon sinks and sources. The primary control on atmospheric CO_2 is the uptake of CO_2 by the ocean, mainly by the processes of the "biological carbon pump" (the combined action of phytoplankton photosynthesis, and the precipitation and subsequent sinking and dissolution of zooplankton and phytoplankton calcium carbonate ($CaCO_3$) shells), as well

as the "solubility pump" (the absorption of atmospheric CO_2 by cooler ocean water masses, followed by the sinking or lateral transport of these masses, preventing re-equilibration with the surface and bringing CO_2 to the intermediate/deep ocean) (Falkowski et al., 2000). Another important process that affects atmospheric CO_2 is the sequestration by terrestrial ecosystems resulting from: 1) autotrophic respiration, or direct respiration, by plants, 2) heterotrophic respiration, or oxidation of plant-derived organic material, and 3) other disturbances that oxidize organic matter, such as fires (Falkowski et al., 2000). It is likely, however, that CO_2-induced global warming will decrease the atmospheric CO_2 sequestration ability of both the oceans, as a result of increased ocean stratification/saturation of the ocean's buffering capacity of CO_2, and of terrestrial plants, as a result of saturation of the foremost carbon-fixing enzyme in plants (Falkowski et al., 2000). Moreover, Cox et al. (2000) proposed that the current net carbon sink by terrestrial plants may become a net carbon source, resulting from widespread climate-driven loss of soil carbon. Considering this probable decrease in the ability of the oceans and the terrestrial biosphere to sequester atmospheric CO_2, a better comprehension of other processes that produce and consume atmospheric CO_2 is essential.

The magnitude of anthropogenic CO_2 emissions, as well as the magnitude and process of oceanic uptake of atmospheric CO_2 are well-defined; however, the magnitude of terrestrial uptake of atmospheric CO_2 is significantly less well-defined (Fan et al., 1998; Cox et al., 2000). This is highlighted by the existence of the so-called "missing carbon sink." The known anthropogenic output of CO_2 to the atmosphere, minus the known uptake of atmospheric CO_2 by the ocean, is significantly less than the known amount of CO_2 that remains in the atmosphere and, therefore, a significant sink of

atmospheric CO_2 is unaccounted for by current carbon cycle budgets. Tans et al. (1990) estimated this missing sink to be as large as 2.0-3.4 gigatons (Gt) of carbon per year from observations of pCO_2 (partial pressure of CO_2) in the atmosphere. This estimate was met with considerable scrutiny. For example, Sarmiento and Sundquist (1992), Siegenthaler and Sarmiento (1993), and Sundquist (1993) argued that the methods of Tans et al. (1990) did not account accurately for a number of variables that would affect estimation of the missing sink, such as sea-surface skin temperature, the net air-sea gas exchange, and the lateral transport of carbon monoxide (CO) in the atmosphere. After corrections based on these proposed calculations, however, it was still determined that a significant missing sink did indeed exist (Sarmiento and Sundquist, 1992; Sundquist, 1993). In addition, Fan et al. (1998) argued that a notable terrestrial carbon sink exists in North America based on multiple atmospheric models and sea-air flux data. It was determined, however, that, although this CO_2 uptake was large enough to be detected, its magnitude remains uncertain and its cause unidentified (Fan et al., 1998). The existence of this missing sink is widely accepted, and a number of hypotheses exist as to the specific cause. A significant amount of scientific research has been directed towards a more accurate carbon budget by accounting for a terrestrial sink of atmospheric CO_2, including by the dissolution of carbonate rocks (Amiotte Suchet and Probst, 1995; Liu and Zhao, 2000; Groves and Meiman, 2001; Liu et al., 2008; 2010; 2011).

2.4 Carbonate Rock Dissolution as an Atmospheric Carbon Sink

A number of scientific studies have focused on describing and quantifying the atmospheric carbon sink by oceanic processes and, as a result, these processes and the magnitude of this atmospheric CO_2 sink have been relatively well-defined. Since the

scientific acceptance of the presence of a "missing carbon sink" from global carbon cycle models, a significant effort has been made in recent years to identify and quantify processes responsible for the discrepancy in these numbers. One area of interest concerning this research has been the contribution of carbonate rock weathering to the atmospheric CO_2 sink.

Carbonate rocks are chemical sedimentary rocks, most commonly either in the form of limestone ($CaCO_3$), or dolomite ($CaMg(CO_3)_2$). These rocks dissolve at relatively high rates when compared to other common minerals such as feldspars or quartz. Dissolution of these rocks (Figure 4) is significantly enhanced by the presence of H_2CO_3 (carbonic acid), which is commonly found in rain and surface water flowing over and through these carbonate rocks as a result of atmospheric and soil CO_2 dissolved in rain and surface water. As atmospheric CO_2 dissolves in water, most of it ends up as the dissolved inorganic carbon species CO_3^{2-} (carbonate ion), HCO_3^- (bicarbonate ion), and $H_2CO_3^*$ (carbonic acid), where $H_2CO_3^*$ is the sum of $H_2CO_3^*$and aqueous CO_2 (Drever, 1997). This can be described by the following reactions:

$$CO_2 + H_2O \Leftrightarrow H_2CO_3^*. \qquad (2.1)$$

As with other weak acids, once this happens, some but not all of the $H_2CO_3^{-*}$ spontaneously disassociates into bicarbonate:

$$H_2CO_3 \Leftrightarrow H^+ + HCO_3^- \qquad (2.2)$$

In turn, some but not all of the bicarbonate simultaneously disassociates into the carbonate ion:

$$HCO_3^- \Leftrightarrow H^+ + CO_3^{2-}. \qquad (2.3)$$

The proportion of each species is primarily controlled by pH, where, at a pH of 7 to 9, most of the inorganic carbon in the ocean and groundwater is in the form of bicarbonate; at high pH values (>9) carbonate predominates (Dreybrodt, 1988). In the pH range of carbonate-dominated waters, however, the concentration of the carbonate ion is generally negligible (White, 2013). The total dissolved inorganic carbon (DIC) is obtained by summing these species. In typical limestone-influenced waters, dissolved inorganic carbon (DIC) can be determined in these settings by measuring HCO_3^-, pH, and temperature, and calculating the other relevant species using appropriate equilibria and activity corrections (Harned et al., 1959; Stumm and Morgan, 1981).

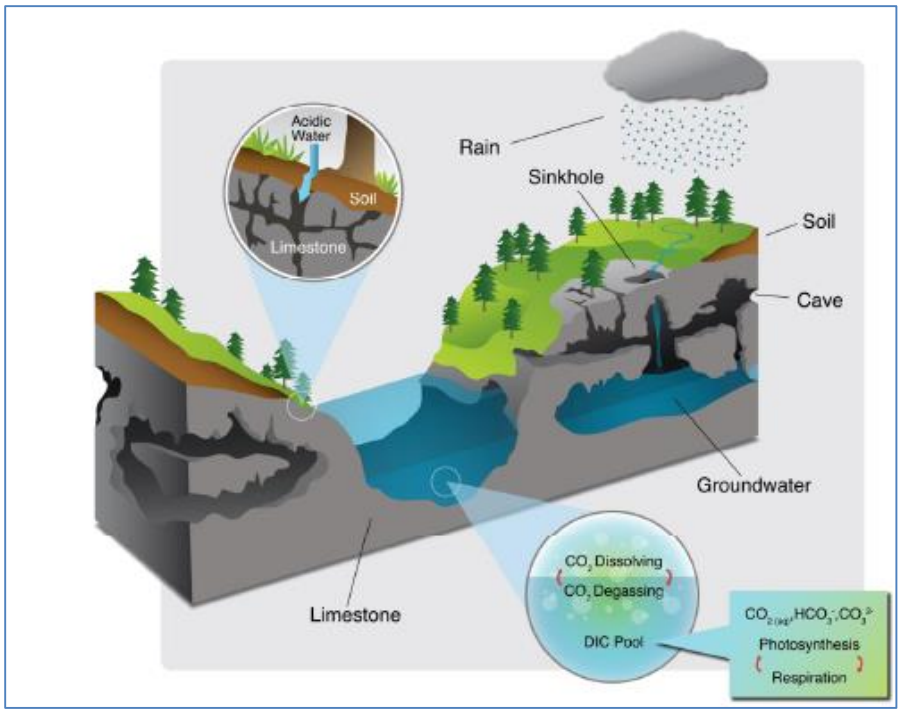

Figure 4: Diagram showing CO_2 processes in carbonate rock landscapes. Source: Created by Jonathan Oglesby, Western Kentucky University, Department of Geography and Geology, after McClanahan (2014).

As the water reaches the ground surface, it typically encounters soil gas with much higher concentrations of CO_2, produced by autotrophic respiration of plants and heterotrophic respiration of organic-derived material; concentrations of the relevant

species and, thus, DIC increase. Taking into account that the carbon in plants originally came from the atmosphere, and considering that the uptake of CO_2 by carbonate weathering decreases soil CO_2 release to the atmosphere, the uptake of soil CO_2 by rock weathering is considered a sink of atmospheric CO_2 (Yuan, 1997; Ludwig et al., 1998; Liu and Zhao, 2000). This weathering of carbonate rocks can be described by the equations:

$$CaCO_3 + H_2CO_3 \leftrightarrow Ca^{2+} + 2HCO_3^- \quad (2.4)$$

and

$$CaMg(CO_3)_2 + 2H_2CO_3^* \leftrightarrow Ca^{2+} + Mg^{2+} + 4HCO_3^-. \quad (2.5)$$

for limestone and dolomite, respectively. In both cases, as evident by the above reactions, for every two moles of carbon produced as HCO_3^-, one mole came from the atmosphere and one mole came from the rock. As a result, the atmospheric sink of inorganic carbon from the atmosphere can be estimated as one half of the total DIC flux leaving a carbonate rock-containing river basin (Jiang and Yuan, 1999; Liu and Zhao, 2000; Groves and Meiman, 2001; Groves et al., 2002; Amiotte Suchet et al., 2003; He et al., 2013). While these reactions dominate the carbonate mineral dissolution process in typical carbonate rock waters, other forward reactions with water and cations also occur (Plummer et al., 1978), and in the presence of strong acids, such as sulfuric acid rain, this source ratio may be affected (Groves and Meiman, 2002). Therefore, the potential for acidification by acid rain should be taken into account when estimating carbon fluxes. Nonetheless, use of this technique has allowed for significant research attempting to quantify the carbon sink effect of carbonate dissolution on scales ranging from relatively

small river basins (*e.g.*, Groves and Meiman, 2001; He et al., 2013; Osterhoudt, 2014), to regional estimates (*e.g.*, Cao et al. 2011; Haryono, 2011), and global estimates (*e.g.*, Liu and Zhao, 2000; Amiotte Suchet et al., 2003; Liu et al., 2010).

Although the dissolution of carbonate rocks acts as an immediate sink of atmospheric CO_2, on geologic timescales, this sink is considered to be balanced by the precipitation of carbonate minerals in the ocean (Berner, 1989; Amiotte Suchet et al., 2003). This takes place in one way as aquatic organisms such as phytoplankton and zooplankton form their shells of $CaCO_{3;}$ while some are dissolved in deeper ocean water, some are buried in sediments (Falkowski et al., 2000). Generally, at least over long time scales such as millions of years, it has been assumed that the process of carbonate precipitation in the ocean effectively balances the atmospheric CO_2 sink by dissolution of carbonate rocks (Berner et al., 1983; Berner, 1989).

More recently, however, this idea has been challenged by pointing out that this assumption does not account for the biological pump of terrestrial and oceanic aquatic organisms, specifically in terrestrial ecosystems where carbon can be diverted into the lithosphere by burial or sedimentation of organic carbon derived by the photosynthetic uptake of DIC (Liu et al., 2010; 2011; Cao et al., 2012; Groves et al., 2012). This view is supported by a number of significant findings. For example, Ternon et al. (2000) determined that fertilization of oceanic waters by outflow from the Amazon River enhanced the biological pump of CO_2, which resulted in up to a 30% lowering of pCO_2 in this area, increasing the atmospheric CO_2 sink potential of the Atlantic ocean. Yang et al. (2008) studied the carbon source-sink ratio of a subtropical eutrophic lake by calculating an overall mass balance and gas exchange/carbon burial balance, and found

the ratio of carbon emission to burial by the lake to be .08, indicating the lake was an effective sink of atmospheric CO_2. Einsele et al. (2001) studied carbon burial in modern lake sediments and found that, although the area of lake basins is only 2% of land surface or 0.8% of the size of the ocean surface, a significant amount of atmospheric carbon is buried in lake sediments, amounting to 0.07 Pg (petagrams) of carbon per year. This translates to more than a quarter of annual oceanic carbon burial, which can be attributed to rapid accumulation of lacustrine sediments and a much higher preservation rate than that of the ocean. Moreover, Cole et al. (2007) estimated the total carbon storage in sediments of global inland waters (including lakes, reservoirs, and rivers) to be 0.23 Pg C y^{-1}, and that only 0.9 Pg C /a of total carbon transported by rivers globally reached the ocean.

Considering the substantial magnitude of these various estimates of carbon, buried in sediments of inland waters, which effectively reduces the amount of carbon reaching the ocean from terrestrial ecosystems, it is unlikely, therefore, that the atmospheric CO_2 sink by carbonate weathering is completely balanced by oceanic precipitation, on human timescales (Liu et al. 2010; 2011). Finally, estimates have proposed, considering that the CO_2 flux by carbonate dissolution is strongly coupled with the hydrologic cycle, that the hydrospheric release of carbonate dissolution-derived CO_2 may have a turnover time roughly the same as the oceanic water cycle--roughly 2000 years. This is compared to the atmospheric CO_2 turnover time of roughly 3-5 years, CO_2 turnover time for plants of roughly 50 years, and decades to 1000s of years for soil. Thus, it has been proposed that the flux by dissolution can be considered part of the carbon sink on relatively short timescales (Cao et al., 2012).Yet, although this may be the case, a

more detailed accounting of the various terrestrial carbon cycle processes and magnitudes of sources/sinks is ultimately needed for accurate carbon budgeting on a global scale (Cole et al., 2007; Liu et al., 2010), which will most likely lead to a better comprehension of how important this sink is over relatively short human timescales.

2.5 Factors Affecting Carbonate Mineral Dissolution Rates

A number of factors can affect carbonate rock dissolution and, therefore, affect the total atmospheric CO_2 sink effect by this dissolution. It has been shown that the primary factor that influences the magnitude of dissolution at the landscape scale of carbonate rock is the volume of water available, which can be attributed as precipitation minus evapotranspiration over the drainage area (Cao et al., 2011; Haryono, 2011), or discharge leaving the drainage area (Groves and Meiman, 2001; White, 2013) depending upon the methods used to estimate the CO_2 sink. For example, Groves and Meiman (2005) found, in their investigation of weathering of the Logsdon River conduit, an underground river in south-central Kentucky, that the inorganic carbon flux of the river correlated linearly with discharge. Although discharge of the highest stage (nearly or completely filling the conduit) occurred less than 5% of the time, this discharge stage was responsible for the largest amount of dissolution, amounting to 38% when compared by individual stage. White (2013) found that, for a number of sinking streams and karst springs (landscapes formed by the dissolution of soluble rocks, often carbonate rocks), carbon fluxes essentially scale with discharge. Similarly, Liu et al. (2008) found that an increase of the atmospheric CO_2 sink by a factor of ~ 2 occurred after a rainfall event, from the increase of water stage and increase in HCO_3^- concentration (attributed to rain water absorption of soil CO_2). Also, He et al. (2013) found that, in measurements of

precipitation over drainage area, as well as discharge and hydrochemical data at an underground river, on a monthly scale the carbon sink amount by dissolution correlated with discharge, and they determined that discharge rather than precipitation was the main controlling factor. Cao et al. (2011) considered that, based on carbonate dissolution rates estimated by limestone tablet corrosion tests, precipitation is the most important controlling factor, as it directly influences discharge. Although both precipitation and discharge are used in various settings and estimates, there is no question about the considerable effect the volume of water available has on carbonate rock dissolution and, therefore, its CO_2 sink effect.

Another important factor that can affect carbonate rock dissolution rates and, therefore, the CO_2 sink is the concentration of CO_2 in soil. Soil CO_2 represents the steady state result of competing processes, such as the rate of CO_2 production by a number of processes including autotrophic and heterotrophic respiration, the rate at which CO_2 is dissolved by infiltration of water, and the rate at which CO_2 diffuses to the atmosphere (White, 2013). It has been shown that subsoil dissolution of carbonate rocks is far greater than dissolution of carbonate rocks exposed to air (Zhang, 2011), as a result of soil CO_2 concentration being much higher than air (ranging from multiple times higher to hundreds of times higher) (Cao et al., 2011). Temperature can be another factor to consider when estimating carbonate mineral dissolution rates. Water in carbonate-dominated regions is particularly sensitive to air temperature changes, which are related to both diurnal (daily) and seasonal environmental fluctuations (Yuan, 1997). This is primarily a result of air temperature influencing water temperature, pH, and the specific conductance (SpC) of water (the measure of a solution's ability to conduct electricity

related to the concentration of dissolved ions) (Zhang et al., 2005). In some cases, when not taking into account hydrochemical data but, rather, weathering rates by the limestone tablet test method, it has been assumed that temperature can be disregarded when estimating sinks if both the soil CO_2 concentration and the level of NPP (net primary production) of carbon by vegetation are accounted for (Cao et al., 2011). In general, however, due to the seasonal variability of carbonate-dominated waters and, therefore, the CO_2 sink effect, the use of high-resolution monitoring of variables such as pH, SpC, temperature, and precipitation, as well as discharge, is necessary in order to estimate accurately the intensity of the CO_2 sink by carbonate weathering for an drainage area (He et al., 2013).

Yet another variable that is proposed as having a significant impact on the CO_2 sink effect by dissolution is distribution of land use within the basin. Liu et al. (2008) determined that reforestation of land enhances carbonate dissolution rates due to an increase in soil CO_2 in forested compared to un-forested land. This consideration has been further investigated. For example, it was shown by Zhang (2011), in a study involving multiple carbonate-dominated areas of China using hydrochemical data as well as limestone tablet test methods, that dissolution rates increased with the level of land-use cover, from (in ascending order) tilled land, shrub land, secondary forest, grassland and, finally, primary forest. It was determined that regeneration of vegetation (e.g., reforestation or afforestation) can enhance carbonate dissolution rates significantly. When dissolution rates for one entire basin by hydrochemical data were compared with individual land-use rates determined by limestone tablet dissolution, it was found that hydrochemical-calculated dissolution rates were lower than that of some specific land

uses, but higher than others. The results also show, however, that when the average rate for all land uses was compared to the total rate for the basin determined from hydrochemical data, the two rates were fairly close. It was determined, therefore, that, dissolution rates calculated by a single land-use pattern were not applicable for estimations of an entire basin constituted by different land-use patterns (Zhang, 2011). While this can be considered as having a significant effect on dissolution rates from one land use to another, further studies of carbonate dissolution rates and their sink effect will help to determine more clearly the effects of land use on the atmospheric CO_2 sink over an entire basin.

2.6 Other Factors Affecting the Carbon Sink by Carbonate Rock Dissolution

While dissolution of carbonate rocks constitutes a sink of atmospheric CO_2, it is important to note that other processes occurring within a carbonate-dominated basin, as well as processes occurring downstream from the basin, can potentially alter the net carbon sink effect by dissolution. One of the primary ways this can happen is by the precipitation of carbonate minerals within the basin (which effectively acts as an atmospheric CO_2 source), such as precipitation of speleothems--mineral deposits found in caves, or tufa-carbonate minerals that are often deposited in springs or at waterfalls. Deposition of tufa generally occurs at liquid-gas boundaries such as discharge points, springs, and drip water points in caves (Jiang and Yuan, 1999). Furthermore, deposition of tufa can be significantly enhanced in carbonate-dominated areas with active faults or geothermal or volcanic activity due to enrichment CO_2 in water (Yuan, 1997; Jiang and Yuan, 1999). In comparing areas of tufa deposits to areas of carbonate dissolution in the carbonate-dominated regions of China, it was determined that the distribution of the

dissolution area was much larger than the distribution area of tufa deposition, indicating that atmospheric CO_2 sink processes have a larger impact than CO_2 sourced from carbonate precipitation (Jiang and Yuan, 1999). White (2013), considered speleothem precipitation in carbonate areas and asserted that speleothem precipitation is not a significant loss in terms of carbon flux for two reasons: 1) only a fraction of total carbon load is deposited as speleothems, and 2) air-filled conduits intercept only a fraction of the water descending from the epikarst (the highly weathered bedrock immediately beneath the soil or at the surface). Another potential loss of carbon to the atmosphere that can occur within a basin is CO_2 degassing or the emission of CO_2 from water to the atmosphere as a result of hydrodynamic conditions or temperature changes. It is contended that degassing in spring-runs (streams fed by the discharge of a spring) can amount to the loss of 5-10% of total carbon load to the atmosphere, while deposition of tufa can amount to a greater loss (White, 2013). Overall, it has been considered that, even though carbonate-dominated systems are leaky in the sense that some of the total carbon sequestered by dissolution can be returned to the atmosphere, the carbon sink effect is predominant (Jiang and Yuan, 1999; White, 2013).

Besides carbon fluxes that can occur within a carbonate rock-dominated basin, which can be accounted for effectively if hydrochemical data are gathered at the basin discharge point, fluxes of carbon can occur downstream from the basin. This potential flux should also be kept in mind when considering the carbon sink effect of carbonate dissolution. As previously discussed, organic carbon derived by the photosynthetic uptake of inorganic carbon by plants can be buried in terrestrial aquatic sediments; in addition, the total flux of carbon to the ocean from carbonate dissolution can be affected

by CO_2 degassing in lakes, reservoirs, rivers and estuaries (Cole et al., 2007). Liu et al. (2010) estimated the mean release rate of carbon to the atmosphere from rivers to be 20% of both internal and external runoff sinks, although they acknowledged that there are large spatial variations in the magnitude of this process. In studying the Hudson River in New York, Raymond et al. (1997) measured a number of parameters, on both spatial and temporal scales, to determine the carbon flux of a specific section of the river. They determined that 70-162 g C m^{-2} yr^{-1} (grams of carbon per square meter per year) were outgassed to the atmosphere over the study period, amounting to 13%-27% of the net input of CO_2. Zhai et al. (2007) conducted a similar study in the inner Changjiang Estuary of the Yangtze River, measuring hydrochemical parameters, and found that the CO_2 degassing level was much lower than some other well-documented urbanized riverine-estuarine systems, with the total degassing of CO_2 amounting to only 2.0-4.6% of the total DIC export of the river. Although it is evident that CO_2 degassing estimates are highly variable spatially, this phenomenon should not be overlooked when considering the net carbon sink effect by carbonate rock dissolution.

2.7 Methods for Estimation and Calculation of Carbonate Dissolution Rates

A considerable number of scientific studies have attempted to estimate carbonate dissolution rates and the carbon sink effect by carbonate dissolution using a number of different methods, depending primarily on spatial scale and availability of data (*e.g.*, Amiotte Suchet and Probst, 1995; Liu and Zhao, 2000; Groves and Meiman, 2001; Amiotte Suchet et al., 2003; Cao et al., 2011; He et al., 2013; Osterhoudt, 2014). One method that has often been used is mathematical modeling of carbonate weathering,

accounting for precipitation or runoff as a variable. For example, Sweeting (1972) derived a formula for dissolution rate of carbonate rocks given as:

$$D_r=0.0043P^{1.26} \qquad (2.6)$$

where D_r is the dissolution rate and P is precipitation. Likewise, Amiotte Suchet and Probst (1995) established a relationship between runoff and a weathering coefficient for different rock types based on statistical data from 232 drainage basins in France, which were compared to observed measurements and tested on three large river basins for validation, given as:

$$F_{CO2}=a\cdot Q \qquad (2.7)$$

where F_{CO2} is the CO_2 consumption rate and a is the coefficient of different rock types. This model, termed GEM-CO_2 has been used in a number of studies (*e.g.,* Ludwig et al. 1998; 1999; Amiotte Suchet et al., 2003). Liu and Dreybrodt (1997) determined that the rate of carbonate dissolution in turbulent CO_2-H_2O solutions can be estimated by a linear rate law, given as:

$$R=a(C_{eq}-C) \qquad (2.8)$$

where R is the dissolution rate, C is the concentration of Ca^{2+}, C_{eq} is the equilibrium concentration of Ca^{2+}, and a is a rate constant, dependent on temperature, pCO_2, thickness of the diffusion boundary layer adjacent to the mineral, and the thickness of the water sheet flowing over the mineral. It has been noted that this approach does not account for potential carbonate reprecipitation that may occur and, therefore, over-estimates values (Liu and Zhao, 2000).

In addition to modeling, other methods have been utilized based on measurement of parameters for calculating the dissolution rate and its carbon sink effect. One frequently used method is the carbonate rock tablet test method, in which a standard limestone tablet of known surface area and insoluble matter content is generally buried or placed on exposed rock in the study area. The tablet is later retrieved and, from the loss of material, the dissolution rate at the selected location can be calculated. This method has been applied in a number of studies (*e.g.*, Jiang and Yuan, 1999; Liu and Zhao, 2000; Cao et al., 2011; Zhang, 2011). Finally, and possibly the most widely used method, is the hydrochemical-discharge method, in which hydrochemical data such as SpC, temperature, pH, and alkalinity, as well as discharge, are used to estimate the total DIC leaving a basin and, therefore, the carbon sink effect by carbonate dissolution. Variations of this technique have been applied in numerous studies (*e.g.*, Jiang and Yuan, 1999; Groves and Meiman, 2001; Zhang, 2011; Haryono, 2011; He et al., 2013; Osterhoudt, 2014).

2.8 Estimates of Carbon Sink by Carbonate Dissolution

Carbonate rocks exposed at the surface constitute a significant portion of the Earth's surface, with estimates of the total area exposed ranging from 12.34×10^6 km^2 (Gibbs and Kump, 1994) to 21.09×10^6 km^2 (Meybeck, 1987), accounting for 9.3% to 15.9%, respectively, of the total continental area given as 133×10^6 km^2 by Dürr et al. (2005). Weathering of these carbonate rocks has been presumed to have a significant effect when considered on a global scale. Numerous studies have estimated the global carbon sink value by carbonate dissolution; however, the values of these estimates can vary significantly. An early estimate made by Berner (1989) was fairly low when

compared to some other estimates at 0.142 Pg C/a. Sarmiento and Sundquist, (1992) obtained an estimate of 0.4 Pg C/a from a global carbon budget; it should be noted, however, that this estimate was made under the assumption that geochemical fluxes were operating in a steady state. Yuan (1997) obtained the greatest published value at 0.608 Pg C/a using a global mean dissolution rate. Liu and Zhao (2000) made use of the carbonate rock tablet method, their linear correlation model, and the DBL model, achieving values ranging from 0.1-0.4 Pg C/a. Using the GEM-CO_2 model and a worldwide 1° x 1° grid lithology map, Amiotte Suchet et al. (2003) estimated a value of 0.104 Pg C/a. Hartmann et al. (2009) provided one of the lowest published estimates at 0.088 Pg C/a, using the global lithology map from Dürr et al. (2005) and a linear bicarbonate model. While it is obvious that the use of different values of total carbonate rock exposed globally affects estimates, the extensive range of estimated carbon sink values (ranging from 0.088 Pg C/a to 0.608 Pg C/a) emphasizes the considerable uncertainties associated with making global estimates. While global estimates can serve to highlight the magnitude and, therefore, importance of the atmospheric carbon sink by carbonate dissolution, the extensive range of estimated values implies that further understanding and investigation of this carbon sink is necessary in order to quantify accurately its extent on a global scale.

In addition to global estimates, a substantial amount of research has been done on a much smaller scale and, to some extent, on a regional scale, to calculate the carbon sink by carbonate dissolution. Generally, these studies have made use of measured data or observed dissolution rates, as opposed to the use of modeling techniques and/or assumed global dissolution rates on the global scale. For instance, He et al. (2013) studied the carbon sink potential of the Banzhai subterranean stream in the Maolan National Nature

Reserve in China, using hydrochemical data gathered at a monitoring station on the stream. They concluded that, because of seasonal variability in the magnitude of the sink, the use of high resolution monitoring technology is crucial to calculate and analyze accurately the intensity of the carbon sink. Similarly, Groves et al. (2002) described the beginnings of a global network of research sites, including Kentucky and California in the U.S., and in China, with an emphasis on collection of high-resolution hydrochemical data in order to better understand and estimate the carbonate dissolution carbon sink. With regards to regional estimations, Cao et al. (2011) obtained a total carbon sink estimate of 1.85×10^6 t C/a (metric tons of carbon per year) for the 452,600 km^2 Pearl River basin in China, using the carbonate tablet test method, and obtaining data on precipitation, soil CO_2 concentration, and NPP of vegetation. Additionally, Haryono (2011) estimated the carbon sink by dissolution of the Genug Sewu Karst on the Indonesian island of Java. Using precipitation data and $CaCO_3$ measurements made at 22 springs, the author found that, for the 1300km^2 area, the total carbon sink was 72,804 t C/a. It should be noted that precipitation data were for the period of 1945 to 2002, and $CaCO_3$ data were taken from studies published in 2002 and 2003, without specification of the temporal range of data.

Groves and Meiman (2001) investigated the carbon sink potential of the Logsdon River, a major subterranean stream in south-central Kentucky. They collected high resolution data on stage, velocity, temperature, and SpC, in addition to water samples, through the use of two observation wells intersecting the river. For the 25km^2 drainage area, it was determined that the total inorganic carbon sink was $7.8 \times 10^3 \pm 1.9 \times 10^3$ kg ha^{-1} (kilograms per hectare) over one hydrologic year. Building upon this work,

Osterhoudt (2014) explored the atmospheric carbon sink of the Green River in south-central Kentucky. Carbon sink values, as well as DIC values, were determined for two drainage basin sections of the river, one nested within the other. Calculations were based on high resolution measurements (15 minute) at two locations of pH, and SpC, as well as discharge from the USGS gaging stations and weekly water sampling for relevant cations and anions. Atmospheric carbon sink values were normalized by time and area of carbonate rock within the respective basins; these values for each of the two basins were found to be in agreement within 12% for the 15-minute data, indicating that this normalization technique can estimate accurately a carbon sink in basins of different size, as well as in different size areas of carbonate rocks. However, sink values calculated by this same method for weekly data were found to agree within 36%, indicating greater noise within the weekly data. The agreement of the values calculated by this normalization technique suggests the possibility of a single technique, which could be used to estimate carbon sink values for numerous rivers, potentially regardless of scale or area of carbonate rock outcrop.

2.9 Conclusions

Current atmospheric CO_2 levels are extensively altered by human activity (Falkowski et al., 2000). Moreover, it is likely that these levels will continue to rise throughout the current century (Hoffert et al., 1998). Taking into account the growing public, political, and scientific concern for climate change, and the strong correlation of atmospheric CO_2 levels with these changes, the need for accurate accounting of carbon sinks and sources is greater than ever. Although the anthropogenic emissions of CO_2 to the atmosphere and the oceans uptake of CO_2 are well-defined, there still exists a

prominent sink of atmospheric CO_2 that is currently unaccounted for in global budgets (Sarmiento and Sundquist, 1992; Siegenthaler and Sarmiento, 1993; Fan et al., 1998). This has resulted in a significant amount of research into the identification and quantification of these poorly characterized processes in the carbon cycle. One area of notable research attempting to aid in this endeavor is the study of the carbon sink effect of carbonate rock dissolution. It has been suggested that the atmospheric carbon sink effect by dissolution of carbonate rocks may play a role in accounting for the "missing carbon sink" of the global carbon cycle (Liu and Zhao, 2000; Liu et al., 2011; Cao et al., 2012; White, 2013). Considering that the contribution of carbonate weathering to the atmospheric carbon sink has been shown to increase with increasing atmospheric CO_2 concentrations (Liu and Zhao, 2000), accurate measurement of this sink is crucial. While a significant amount of research has attempted to quantify this sink on a global scale, estimates can vary significantly. Furthermore, even as a number of studies have worked to estimate this sink over smaller scales, further work to improve methods of estimation and, therefore, improve the precision of estimates is still needed (Liu and Zhao, 2000; Cao et al., 2011).

Studies regarding the carbonate dissolution-carbon sink effect in the south-central region of Kentucky have indicated that these carbonate areas indeed function as an atmospheric carbon sink. The work of Osterhoudt (2014) demonstrated that the method of normalization of carbon sink values by time and area of carbonate rock, can estimate accurately these values in different basins, effectively normalizing measurements for differences in size and amount of carbonate rock within the basin. This method potentially could prove to be of use in a multitude of settings if it can be validated by

generating carbon sink values in other river basins that are in agreement with the values already established. The employment of this method to existing freely available data could substantially broaden its application because, while high-resolution data collected from established monitoring sites are ideal, obtaining these data for numerous locations is generally not practical. Also, if it can be shown that values ascertained by this method are in agreement across basins, based on the measurements previously taken into account, this should demonstrate effectively that other factors that could potentially impact the carbon-sink effect, such as land use, precipitation distribution, carbonate re-precipitation, etc., may essentially only constitute noise. Therefore, application of this method to other basins for validation, as well as application to existing data, is necessary in order to determine the potential for its widespread use in other settings.

Chapter 3: Study Area

3.1 Introduction

The Barren River in south-central Kentucky is a major tributary of the Green River (Figure 5), which is, in turn, a major tributary of the Ohio River. The Barren and Green converge near Morgantown, Kentucky, at the border of Barren and Butler counties. Its drainage basin is primarily in Kentucky, with a relatively smaller portion in the northern part of central Tennessee, and it encompasses an area of 4,789 square kilometers (USGS 2014a). The drainage basin is situated within the Interior Low Plateaus Physiographic Region of the U.S., which extends from the Appalachian Mountains in the east to the Mississippi River in the west and is bounded in the south by the Mississippi Embayment, and in the north by the southern extent of continental glaciation. The most well-developed karst landscapes of the United States are found within this region (Palmer and Palmer, 2009). More specifically, the drainage basin is within the Mississippian Plateau, defined as the Pennyroyal Plateau in Kentucky.

In addition to study of the Barren River drainage basin, the upper Green River drainage basin upstream from Greensburg, Kentucky, was considered upon completion of initial analysis of the Barren River drainage basin (Figure 6). This was needed in order to obtain an additional dataset for carbon flux calculations from existing data, for both another hydrologic year of data as well as for the period of study by Osterhoudt (2014), who studied the upper Green River drainage basin. The Upper Green River drainage basin, upstream from Greensburg, Kentucky, is primarily underlain by Mississippian-aged limestones and Mississippian and Devonian-aged shales (Osterhoudt, 2014), with carbonate rocks constituting a much lesser percentage of the drainage area when compared to the Barren drainage basin upstream from Bowling Green. Further study area

description focuses on the Barren River drainage basin, although a detailed description of Upper Green River basin geologic setting has been provided by Osterhoudt, (2014).

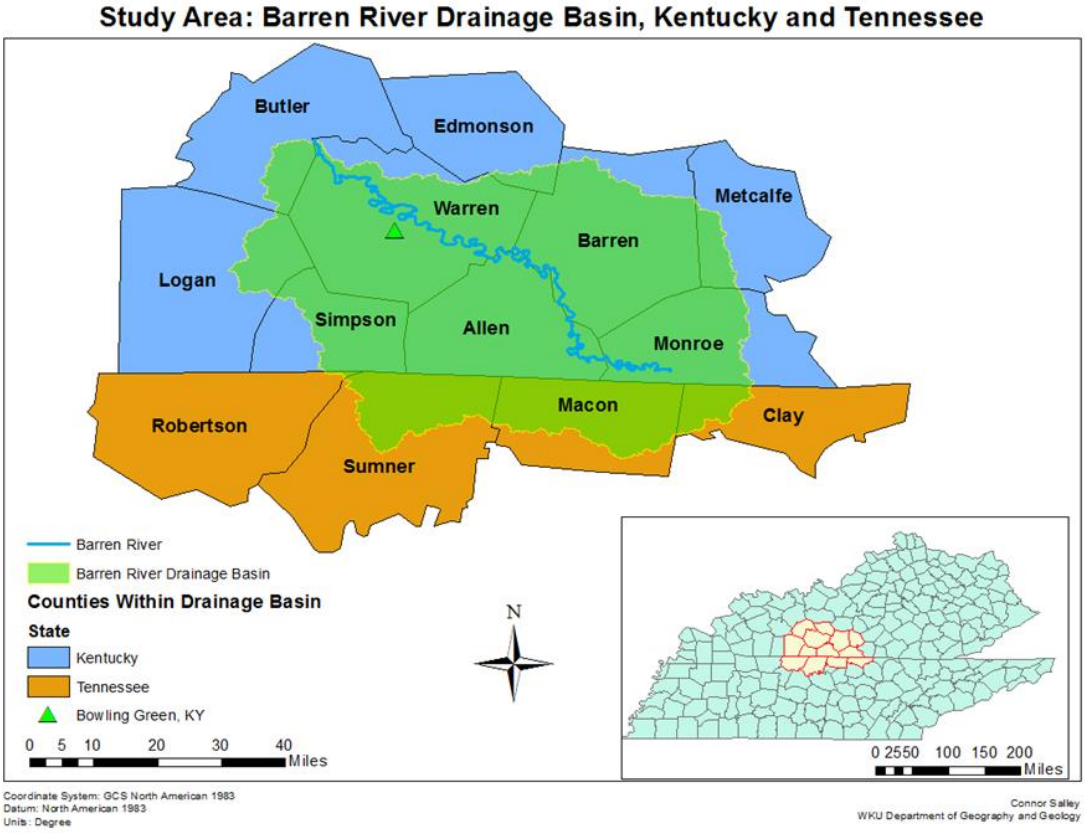

Figure 5. Study Area: Barren river drainage basin, Kentucky and Tennessee.
Sources: Created by the author from USDA (2014) and USGS (2014b) data.

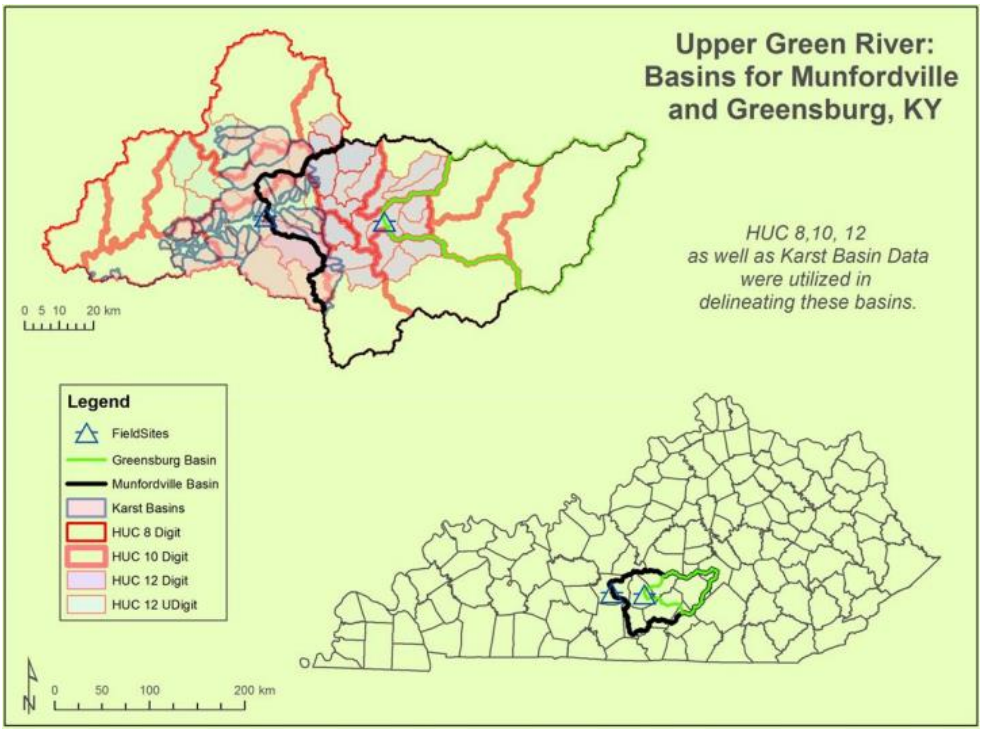

Figure 6. Upper Green River: Basins for Munfordville and Greensburg, KY.
Source: Osterhoudt (2014).

3.2 Physiographic and Geographic Setting

The Barren River and Green River drainage basins are situated within the Pennyroyal Plateau in Kentucky (Figure 7) and the Highland Rim in Tennessee. The Pennyroyal Plateau is an upland region underlain by Mississippian rocks, most of which are limestone (Sauer et al., 1927). The physiographic region is bounded by the Cumberland Plateau or Eastern Kentucky Coal Field in the east, the Western Kentucky Coal Field or the Mississippi Embayment in the west, The Knobs or the Ohio River in the north, and it continues to the south into Tennessee (Newell, 2001). Within the Pennyroyal Plateau region, a large upland plain exists that is characterized by tens of thousands of sinkholes, sinking streams, dry valleys, springs, and caves (KGS, 2012). In this area, surface drainage features are poorly developed because of the extensive network of subsurface

rivers and streams, formed by the weathering of limestone (Newell, 2001). The region is drained primarily by the Green River and its tributaries, with the river valleys and karst drainage network subtly controlled by the regional dip of the limestone beds to the northwest, away from the Cincinnati Arch (Newell, 2001). The Barren River drainage basin lies within the Kentucky counties of Allen, Barren, Butler, Edmonson, Logan, Metcalfe, Monroe, Simpson, and Warren, and the Tennessee counties of Clay, Macon, Robertson, and Sumner. The largest city within the drainage basin is Bowling Green, KY, while smaller cities or towns within the basin include Glasgow, Franklin, and Scottsville, KY, and Portland and Lafayette, TN.

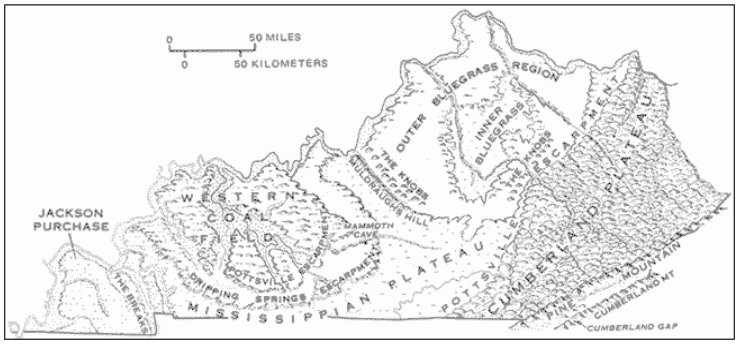

Figure 7. Map of Kentucky physiographic regions. Source: Newell (2001).

3.3 Barren River Geologic Setting

The predominant rock type within the drainage basin is limestone, underlying the majority of the area. Other rock types that occur are dolomite, siltstone, shale, black shale, and sand as alluvium, all to a much lesser extent. Rocks within the drainage basin are primarily Mississippian in age, with some Silurian, Devonian, Ordovician, and Pennsylvanian-aged rocks, again to a much lesser extent. The Mississippian-aged rocks, which dominate basin lithology, are of the Mississippian System. This system is represented mainly by marine sedimentary rocks that underlay the Appalachian and

Illinois Basins and originally extended across the entire state (Grabowski, 2001). These rocks were formed during a widespread shallowing of seas during Mississippian time, in which basinal and deltaic shales were deposited, followed by shelf limestones and dolomites as well as coastal sandstones and shales (Grabowski, 2001). Geologic structural deformation is limited, with a slight regional dip to the northwest of one to one-and-a-half-degrees (Meiman, 2006) away from the Cincinnati Arch, a prominent regional uplift feature that extends from the Nashville Dome in Tennessee to northwestern Ohio (McDowell, 2001).

The primary geologic units (Figure 8) within the drainage basin are the St. Genevieve and St. Louis Limestones (Mgl), undifferentiated Salem, Warsaw, and Harrodsburg Limestones (Msh), and the undifferentiated Renfro and Muldraugh members of the Borden Formation and Fort Payne Formation (Mbf). The St. Genevieve Limestone ranges from 57- to 97-meters thick and is divided into three members. The basal member is the Fredonia Limestone, a very light gray, massive, crossbedded, oolitic to skeletal limestone; overlying this member is the Rosiclaire Sandstone, composed of calcareous sandstone and shale; and overlying the Rosiclaire is the Levias, a skeletal to oolitic limestone that is similar to the Fredonia. The St. Louis is a very fine-grained, somewhat cherty, argillaceous and dolomitic limestone with a 3-6-meter-thick zone of extremely cherty limestone near or at the top (Grabowski, 2001). The Salem and Warsaw Limestones are a mix of argillaceous, cross-bedded limestone and dark, dolimitic siltstone and shale, and cannot be differentiated everywhere from each other; thus, they are combined into a single map unit (Grabowski, 2001). The Harrodsburg is a light-gray, crossbedded, cherty skeletal limestone and is normally 3.5-6 meters thick. The silty, and

cherty dolomitic section of the Borden Formation is classified as the Muldraugh member, while the sandy and silty dolomite and limestone section is classified as the Renfro Member. Finally, the Fort Payne Formation is a mixture of gray to black dolomitic siltstone and cherty dolimitic limestone and is as much as 201 meters thick in south-central Kentucky (Grabowski, 2001). Stratigraphically, the lowermost of these lithologies is the Fort Payne/Borden Formations, which are overlain by the Harrodsburg Formation and, is in turn, is overlain by the Salem/Warsaw Formations. The St. Louis Limestone overlays the Salem/Warsaw Formations and, finally, the St. Genevieve is the uppermost of the primary formations, overlying the St. Louis (Palmer, 1981).

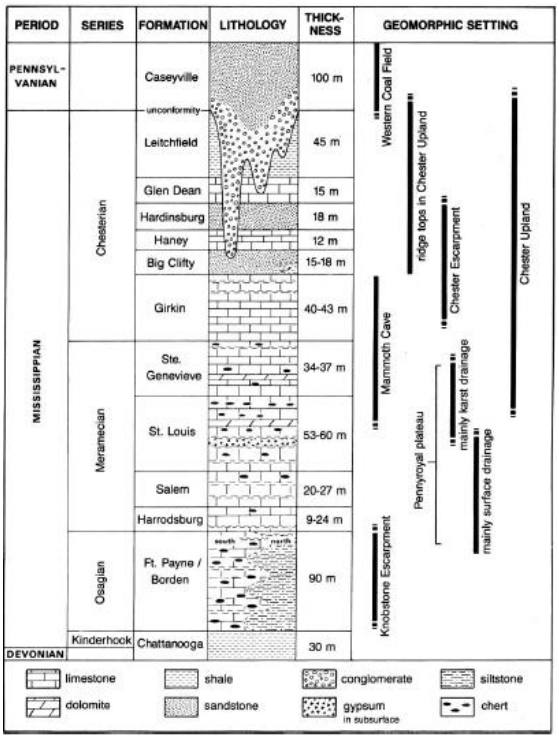

Figure 8: Stratigraphic column showing the major regional geologic units. Source: Palmer, 1981.

3.4 Hydrologic and Climatic Setting

Climate within the study area is classified as Humid Subtropical (Köppen-Geiger Cfa) (Peel et al., 2007). Mean annual temperature in southern Kentucky is 15°C, with high temperatures exceeding 32°C an average of 40 or more days a year and low temperatures dropping below -18°C only 2 days a year on average (KY Climate Center, undated). Precipitation across Kentucky is generally well-distributed temporally, with fall being the driest season, and spring being the wettest, while mean annual precipitation in southern Kentucky is 1,320 mm (KY Mesonet, 2016). Drainage within the Barren River water shed is primarily subsurface flow within the karstic areas of the northern portion of the basin, while surface drainage dominates the southern portion. Where subsurface flow dominates, flow paths and groundwater drainage divides have been well defined as a result of previous fluorescent dye-tracing studies. The Barren River is impounded roughly 16 kilometers east of Scottsville, KY, forming the Barren River Lake, with a drainage area upstream from the dam of 2,435 km^2, and a maximum storage area of 8,154 hectares (Barrenriverlake.net, 2014).

Chapter 4: Methodology

4.1 Introduction

Investigations of the atmospheric carbon sink and related carbon fluxes resulting from carbonate rock dissolution have generally made use of three types of methods. Some studies (primarily global or large scale) have used mathematical/geochemical modeling and extrapolation of observed or calculated dissolution rates (e.g., Amiotte Suchet and Probst, 1995; Liu and Zhao, 2000; Amiotte Suchet et al., 2003). Other studies have used observed dissolution rates of carbonate rock tablets to make estimations of the carbon sink effect (e.g., Jiang and Yuan, 1999; Cao et al., 2011; Zhang, 2011). Another method, which has been called the hydrochem-discharge method, may be the most widely utilized. This method makes use of high resolution water chemistry data, and spring or river discharge leaving a drainage basin, to determine the carbon sink for that drainage area (e.g., Groves and Meiman, 2001; Haryono, 2011; He et al., 2013; Osterhoudt, 2014). Furthermore, He et al. (2013) proposed that the use of high-resolution monitoring data is necessary in order to estimate accurately the carbon sink effect by carbonate rock dissolution.

Measurement of the atmospheric carbon sink from carbonate mineral weathering involves two steps: 1) measuring the flux of associated inorganic carbon leaving a defined drainage system, and 2) partitioning the inorganic carbon sourced from the atmosphere and also from the rock. This study is focused on developing methods to better measure the first of these: the inorganic carbon flux over large river basins. It utilized a variation of the hydrochemical discharge method, as described by Osterhoudt (2014), to estimate the atmospheric carbon flux values for the Barren River, south-central Kentucky

and, subsequently, the upper Green River basin upstream from Greensburg, Kentucky. Using this method, the dissolved inorganic carbon (DIC) flux over a hydrologic year for each basin was calculated from water chemistry data and then normalized by time, area of carbonate rock within the basin, and the amount of water available for carbonate rock dissolution measured as precipitation minus evapotranspiration over the area of carbonate rock. This study utilized existing water chemistry data provided by Bowling Green Municipal Utilities (BGMU) and Greensburg Water Works (GWW), and discharge data from the Bowling Green USGS gaging stations. In addition, existing GIS and weather station data have been used for mapping, including basin delineation, carbonate rock area calculation, and precipitation calculation. Data were obtained from the Kentucky Geological Survey Geospatial Data Library (KGS, 2014), the KY Mesonet (2016), the Midwest Regional Climate Center Cli-MATE Online Data Portal (MRCC, 2016), the United States Department of Agriculture National Resource Conservation Service Geospatial Data Gateway (USDA, 2014), and the USGS National Hydrography Dataset Watershed Boundary Database (USGS, 2014b).

4.2 Water Chemistry and Discharge Data

Water chemistry data were acquired from the water quality laboratory at BGMU and GWW, while discharge data were obtained from the US Geological Survey (USGS, 2014a). The USGS gaging station 03314500-Barren River at Bowling Green, KY, and the BGMU Water Treatment Plant (WTP), as well as the USGS 03306500 Green River at Greensburg, Kentucky (USGS, 2016) and the GWW, are located adjacent to each other on the Barren and Green rivers, respectively, ensuring that discharge data coincide with water chemistry data. Barren River data were obtained for the period of October 1, 2012

through September 30, 2013. This study period was chosen as it is the most recent complete year of discharge data available from the USGS for the Bowling Green gaging station. Data obtained for the upper Green River were from February 1, 2013, to January 31, 2014. This study period was chosen as it was the most recent hydrologic year of discharge data available that coincided with the study period used by Osterhoudt (2014). Discharge for both stations is based on automatic measurements of stage height over 15-minute intervals, (USGS, 2014a); thus, discharge data used are at a 15-minute-resolution. Direct discharge data were acquired from the Bowling Green gaging station, while only stage height data were available at Greensburg, and required conversion to discharge values using the formula for a rating curve (Osterhoudt, 2014). Water chemistry data are from raw (untreated) water collected and analyzed every eight hours at BGMU, and once per day at GWW, yielding water chemistry data of eight-hour and daily resolutions, respectively.

Raw water samples were collected by BGMU and GWW and were analyzed in laboratories at each location. Water chemistry data provided for this study include pH, temperature, and total alkalinity. Water samples are analyzed for these parameters using Standard Methods for the Examination of Water and Wastewater (SM), United States Environmental Protection Agency (EPA) methods, or HACH, Inc. methods (HACH, 2012), which either operate directly based on a Standard Method or demonstrate a method considered to be equivalent by the judgment of the EPA (Gott, 2014). Water pH is measured following the HACH method #8156 (equivalent to EPA method 150.1 and SM 4500-H+B), which use a pH meter and electrode to measure sample pH (HACH, 2012). Water temperature is measured according to SM 2550 using a thermometer (SM,

2006a). The total alkalinity of water is determined according to SM 2320B, involving titration of the sample with standard sulfuric or hydrochloric acid (SM, 2006b).

4.3 Precipitation Measurement

Precipitation and surface air temperature data were acquired from the KY Mesonet (2016), and the Midwest Regional Climate Center Cli-MATE Online Data Portal (MRCC, 2016). In both cases, data acquired were mean monthly temperature and monthly cumulative precipitation measured at individual weather stations. Stations were chosen based on location and availability of required data for the correct time period. These were chosen both within the basin and immediately surrounding the basin, in an attempt to eliminate edge effect or the loss of relevant data due to study area placement (Figure 9). Mean monthly temperature data were required to calculate the monthly potential evapotranspiration, then subtracted from cumulative precipitation to determine the amount of water available for carbonate rock dissolution during the study period. Data were acquired directly from the Kentucky Mesonet website (KY Mesonet, 2016) or the MRCC Cli-MATE Data portal (MWRCC, 2016) and input into Excel spreadsheet software for data management. All data were acquired in or converted to metric units (cm and degrees Celsius) for Potential Evapotranspiration calculation. This was calculated according to the Thornwaithe Equation for potential evapotranspiration (Thornthwaite, 1948):

$$PET = 1.6\left(\frac{L}{12}\right)\left(\frac{N}{30}\right)\left(\frac{10T_a}{I}\right)^{\alpha} \qquad (4.1)$$

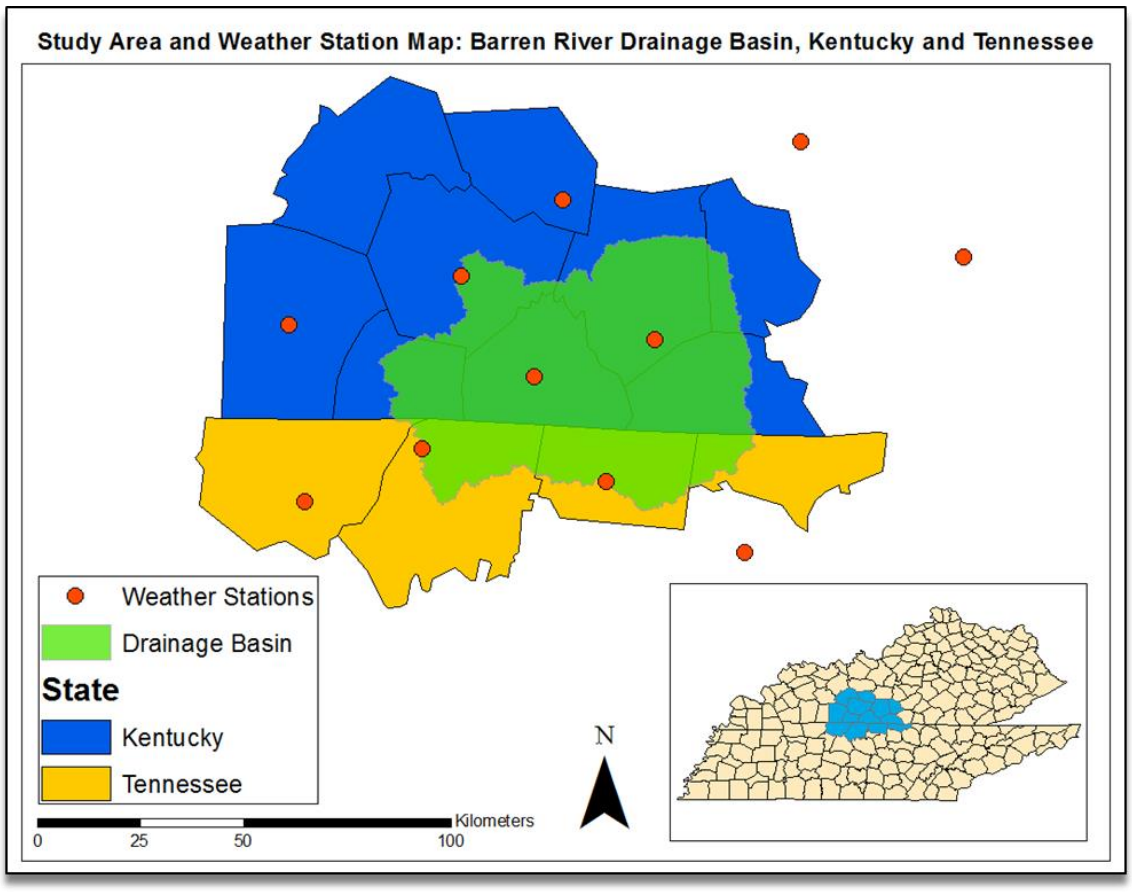

Figure 9. Study area and weather station map: Barren River drainage basin, Kentucky and Tennessee. Source: After MRCC, 2016.

where PET is the estimated potential evapotranspiration, T_α is the average daily temperature (degrees Celsius; if this is negative, the 0 is used) of the month being calculated, *N* is the number of days in the month being calculated, *L* is the average day length (hours) of the month, *I* is a heat index determined by the average monthly temperature, and α is determined from *I*. This was carried out through the use of the San Diego State University online hydrology calculator for the Thornthwaite PET equation (SDSU, 2016). Once the PET had been calculated for each month at each station, it is used to represent values of ET, which were then subtracted from the corresponding cumulative monthly precipitation at each station to determine the P-ET.

These data were input into ArcGIS 10.1 in order to map the interpolated precipitation minus evapotranspiration for the entire basin. Interpolation of the existing point data is required because the depth of precipitation falling at a specific weather station is only representative of that point in space; interpolation generates multiple values, as specific points in space between observed data points based on distance between these specific generated points in space and the observed data points. Interpolation for the full hydrologic year of cumulative P-ET values was carried out using both Inverse-Distance Weighted (IDW) and Kriging techniques to determine a value of average P-ET over the entire basin. These tools generated an interpolated raster surface, which is a statistical estimate of precipitation depth over the entire process area. The process area used was slightly larger than the drainage basin, to eliminate edge effects, and the resulting surface was then clipped to coincide with the exact drainage boundary. The average depth of precipitation minus evapotranspiration for the drainage basin was determined from the resultant interpolated surfaces.

4.4 Carbonate Rock Area Calculation

Geologic map data and the delineated drainage boundary data were utilized in this study in order to calculate the area of carbonate rock within the drainage basin upstream from the sampling location. Geologic map GIS data for the part of the basin within Kentucky were acquired from the Kentucky Geological Survey (KGS, 2014), and from the United States Department of Agriculture, National Resource Conservation Service Geospatial Data Gateway (USDA, 2014) for the portion in Tennessee. These geologic data were input into ArcGIS 10.1 in order to map the carbonate rock area.

The geologic map data for each state were combined to form a single GIS layer, according to geologic formation name. This layer was then clipped by delineated drainage basin layer, resulting in a new map layer showing the geology only within the basin. When creating the carbonate rock map, formations classified as "limestone" or "dolostone" according to the Kentucky geologic map (as the majority of the drainage basin is within Kentucky) were considered to be carbonate rock. Where different formations have different classification abbreviations in each state, care was taken to ensure that formations were classified accurately in the newly created map by individually selecting each specific polygon, one at a time, by formation name, in the map's attribute table. All geologic formations designated as carbonate rock were assigned a new attribute to reflect this. These were then selected and a new map layer was created in which all carbonate rocks are a single map unit (Figure 10). The total area of this unit was calculated, resulting in the value of carbonate rock area within the drainage basin.

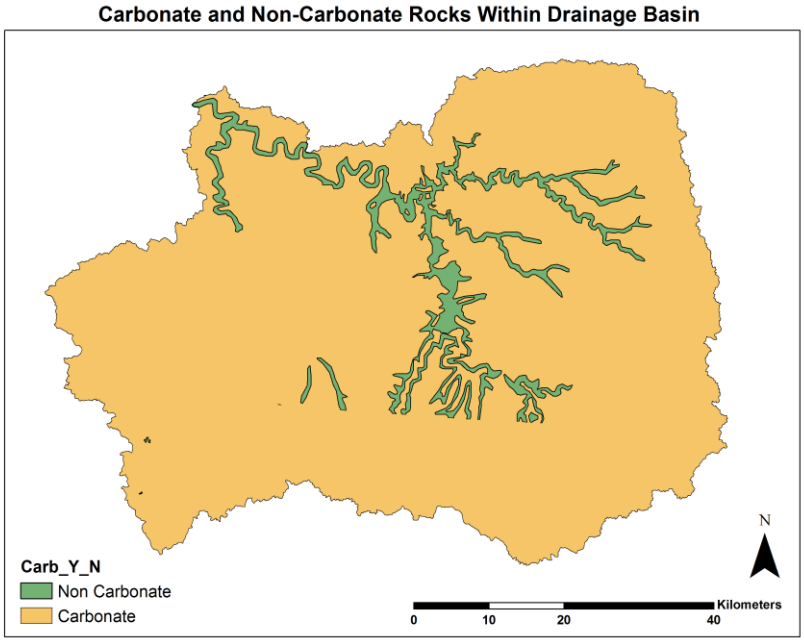

Figure 10. Carbonate and non-carbonate rocks within drainage basin.
Source: Created by the author from KGS (2014) and USDA (2014) data.

4.5 Drainage Basin Delineation

The Barren River drainage basin upstream from the USGS gaging station/BGMU WTP in Bowling Green was delineated using existing GIS data. A new drainage basin boundary map was created by using the current eight-digit Hydrologic Unit Code (HUC) watershed boundary database (USGS, 2014b), as well as topographic 7.5 minute quadrangle maps and Karst Atlas Groundwater Basin Maps (KGS, 2014). Delineation of the drainage basin upstream from the sampling location was necessary in order to calculate the carbonate rock area and precipitation within the drainage boundary. This can often be done using topographic maps and surface drainage boundaries, due to known subsurface drainage features in the basin; however, other data must also be utilized in delineation (Figure 11). Subsurface drainage boundaries and flow paths within the basin have been identified as the result of numerous fluorescent dye tracing studies. Multiple areas where the basin boundaries determined by subsurface drainage were identified as superseding the topographic drainage boundaries, from small sinkholes along the basin boundaries to a relatively large known subsurface river's drainage basin, which discharges into the Barren River downstream from the sampling location (Figure 12). Identification of these drainage features impacted the final delineated basin substantially. Additionally, these subsurface drainage basins were delineated at a much smaller scale than optimal for this study. As a result, these subsurface drainage basins were delineated at a larger scale during basin delineation, using topographic maps and WDB HUC 6, 8, 10, and 12 drainage lines, where applicable.

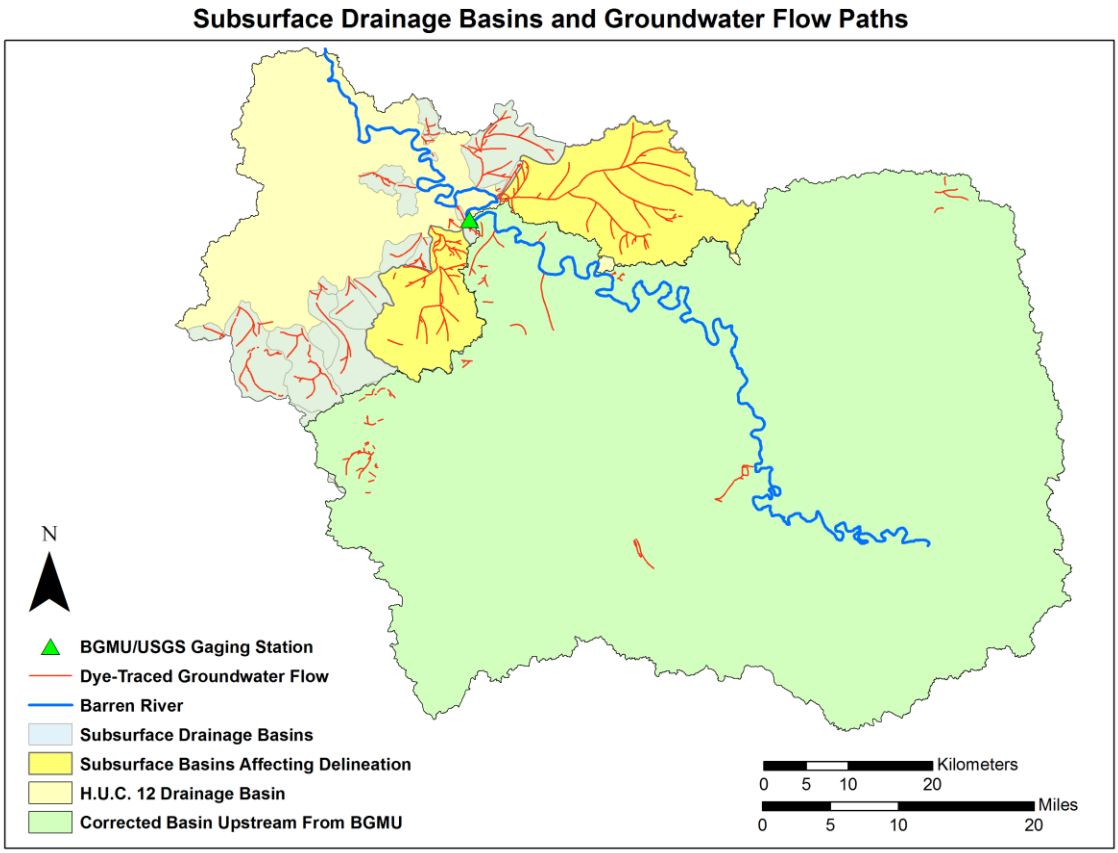

Figure 11. Subsurface drainage basins and groundwater flow paths.
Source: Created by the author from KGS (2014) and USDA (2014) data.

Delineation was carried out using ARCGIS 10.1 Draw and Editor functions to create points and, later, polygon shapefiles. This involved using the existing upstream boundaries where possible, and then digitizing where traditional hand-delineated lines would be on a paper map, where necessary. This method was utilized, as opposed to the use of elevation data and more sophisticated GIS tools, because automated drainage divide calculation tools cannot delineate accurately across closed depressions (sinkholes, dolines) or simultaneously account for subsurface drainage, which is a different data set altogether from the elevation data used for these types of tools. The topographic, HUC,

and Karst Atlas datasets, however, can be viewed and interpreted simultaneously, and the basin was delineated as accurately as possible within the limitations of the basin scale.

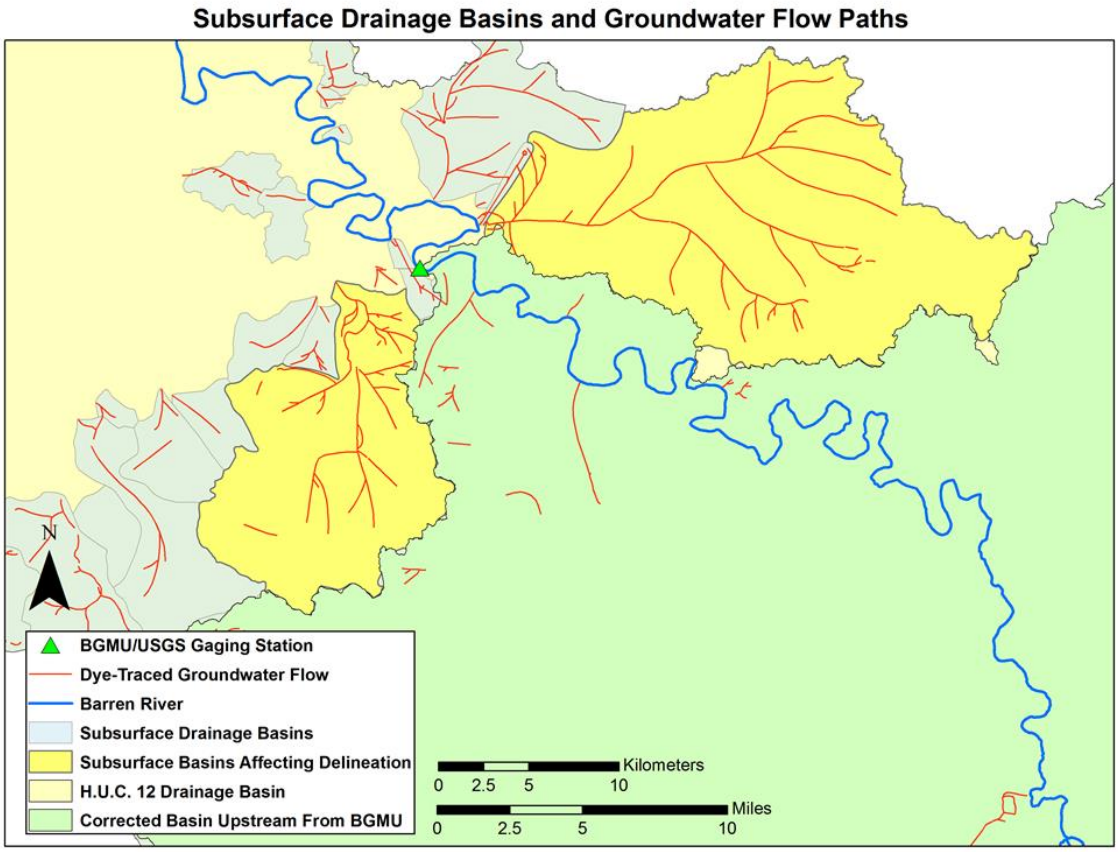

Figure 12. Subsurface drainage basins and groundwater flow paths.
Source: Created by the author from KGS (2014) and USDA (2014) data.

4.6 Carbon Flux Calculation

The total carbon flux of dissolved inorganic carbon (DIC) was measured for the Barren River drainage basin upstream from Bowling Green, Kentucky, for the one-year study period. This atmospheric carbon flux value was then normalized following Osterhoudt (2014) by dividing the total flux by area of carbonate rock and time of study period in days. In addition, the carbon flux value obtained was further normalized by taking into account the amount of available water moving through the system during the

period, measured as precipitation minus evapotranspiration. Furthermore, the value obtained by this process has been compared for validation with the values obtained by Osterhoudt, (2014), and additional values calculated through the use of existing data for the Green River drainage basin upstream from Greensburg, Kentucky.

Discharge data were acquired directly from the U.S. Geological Survey (USGS, 2014a) for the Barren River for the study period, at 15-minute resolution, and reported in values of cubic feet per second (ft^3/s). These discharge data were then processed in order to be combined with water chemistry data, to calculate the DIC flux for the river. Although the Barren River study period was the most recent continuous year the gaging station was active, a small percentage of data was missing, likely due to mechanical difficulties, resulting in lack of measurements for those time periods. Of the 35,040, 15-minute measurements used for the full year, 897 15-minute periods were missing data, amounting to 2.56% of the dataset. These were primarily short 1-hour periods, with occasional longer periods, the longest of which was about 64 hours. Missing data periods were estimated using a linear average between the last measurements made before data loss and the first measurement after, which simply involves division of the difference in measurement value by the number of missing measurement values. This should give a close estimate of the occasional missing values.

Once the missing data were estimated, the discharge values were then converted from ft^3/s to cubic feet per fifteen minutes. The discharge value recorded once every 15 minutes represents the amount of water leaving the basin every second, for that 15-minute period. As a result, the total volume of water leaving the basin during that period is found by multiplying the amount of water leaving the basin per second (discharge in

ft^3/s) by the number of seconds in 15 minutes (900). These values of ft^3/15min were then aggregated to values of cubic feet per eight hours (ft^3/8hr), in order to coincide with each eight-hour period that represents the resolution of the water chemistry data. This was accomplished by directly summing the 96 discharge values representative of each eight-hour period, resulting in the volume of water leaving the basin for each eight-hour period, ft^3/8hr. These values were then converted to liters per eight hours (L/8hr), for use in calculations with water chemistry data.

Alkalinity, pH, and temperature data were acquired from the BGMU water treatment plant and GWW and processed in order to calculate total dissolved inorganic carbon (DIC) values. Water alkalinity is defined as the equivalent sum of the bases that are titratable with a strong acid (Stumm and Morgan, 1981). In carbonate rock-dominated natural waters, although non-carbonate sources of alkalinity may exist, these are very small in comparison to the carbonate species (Stumm and Morgan, 1981; Drever, 1988) and are assumed to be negligible. Therefore, alkalinity can be considered as the sum of the relevant carbonate species CO_3^{2-} (carbonate ion) and HCO_3^- (bicarbonate ion). The proportion of each of these species is primarily controlled by pH, where at a pH of 7 to 9, the majority of inorganic carbon is in the form of HCO_3^- (Dreybrodt, 1988).

Alkalinity data were reported as concentration values, in milligrams per liter (mg/L) of calcium carbonate ($CaCO_3$). These values were then converted into HCO_3^- values by multiplying the value in $CaCO_3$ by 1.22, because one mole of divalent Ca^{2+} is associated with two moles (thus 1.22 grams) of HCO_3^-. Using this value of bicarbonate, using appropriate equilibria and activity corrections based on sample pH and temperature, the total DIC, or the sum of the relevant carbonate species: bicarbonate, carbonate, and

carbonic acid can be calculated (Harned et al., 1959; Stumm and Morgan, 1981). This process was carried out using Systat Sigmaplot 11.0 using the following equilibria:

$$[H_2\ CO_3{}^*] = \frac{[H^+][HCO_3{}^-]}{K_1} \qquad (4.2)$$

and

$$[CO_3^{2-}] = \frac{K_2[HCO_3^-]}{[H^+]} \qquad (4.3)$$

where brackets denote species activities, K_1 and K_2 are temperature-dependent equilibrium constants, and $H_2CO_3{}^*$ is the sum of H_2CO_3 and aqueous CO_2 (Harned et al., 1958; Stumm and Morgan, 1981). These inorganic species are then summed to obtain the total DIC where:

$$DIC = [CO_3^{2-}] + [HCO_3^-] + [H_2CO_3{}^*]. \qquad (4.4)$$

The total DIC flux was then obtained using the eight-hour, or daily resolution DIC concentration values, and the aggregated discharge values in ft^3/8hr. The DIC concentration values in moles per liter (mol/L) representative of each eight-hour or daily period was multiplied by the corresponding discharge value in L/8hr, resulting in a value of the total DIC flux for each eight-hour or daily period in moles. These values were converted using the molecular weight of carbon, resulting in flux values of grams per eight hours, or per day. All eight-hour and daily values for total mass of DIC leaving the basin were then summed for each hydrologic year to calculate the total DIC flux for each study period. Finally, the total DIC flux was then normalized by time (days), area of carbonate rock (km^2) and the volume of water available for carbonate rock dissolution, calculated from precipitation depth falling over the area of carbonate rock.

Chapter 5: Results and Conclusions

5.1 Basin Delineation and Geologic Mapping

The Barren River drainage basin upstream from Bowling Green (Figure 13) was delineated for the purposes of geologic mapping to calculate the area of carbonate rock, as well as precipitation mapping to calculate the cumulative precipitation minus evapotranspiration within the basin. The delineated drainage basin was found to be 4247.7 km^2, or 75% of the entire 5664 km^2 basin of the Barren River to its confluence with the Green River. Two groundwater sub-basins were identified to be discharging downstream from the sampling location, both of substantial size in relationship to the total drainage basin. These groundwater drainage basins were found to be 312.3 and 152.3 km^2 respectively, amounting to a total of 464.6 km^2 or 10.9% of the basin upstream from Bowling Green. While this is a substantial percentage of the drainage area, it should be noted that it is unlikely that the entirety of this area would have been included in the basin upstream even if only topographic and/or elevation data had been used for delineation. This difference in area, however, illustrates still the need for the use of groundwater drainage data when accurate drainage area delineation is required in regions with known subsurface drainage and divides in the subsurface that don't correlate with surface topography.

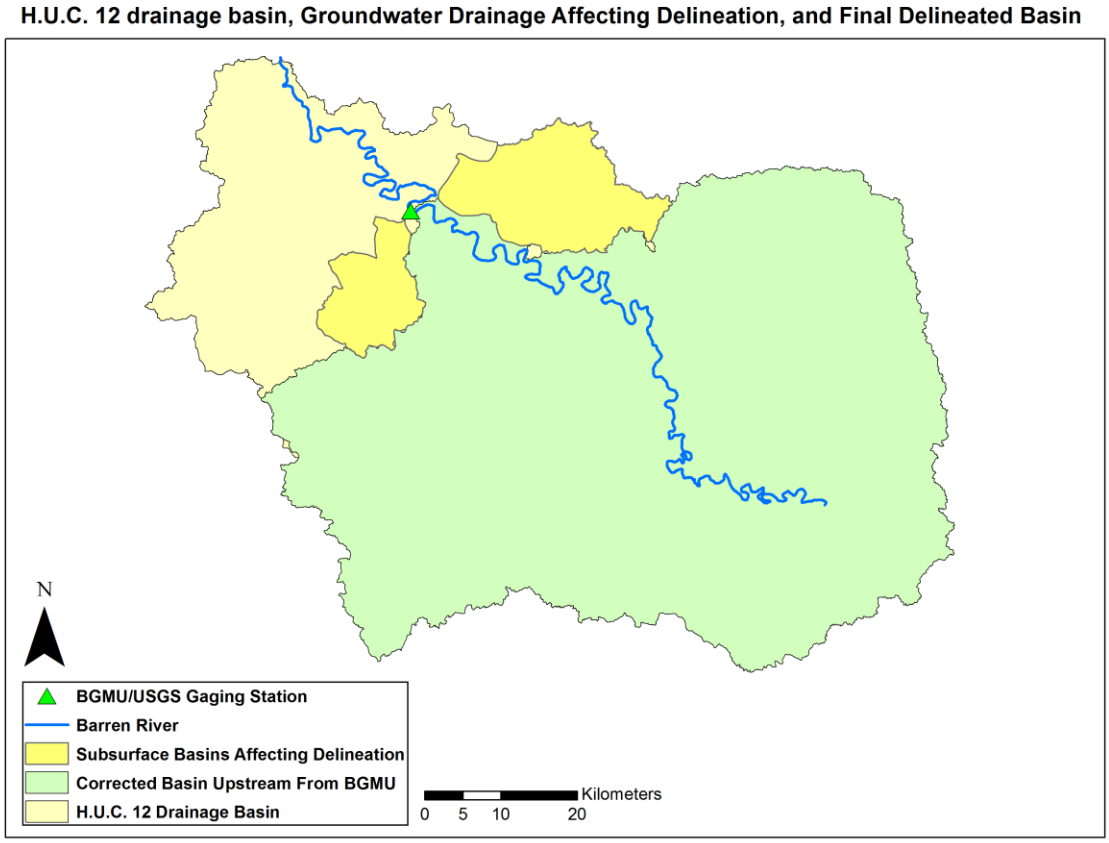

Figure 13. H.U.C 12 drainage basin, groundwater drainage affecting delineation, and final delineated basin. Source: Created by the author from USGS (2014a), KGS (2014), and USDA (2014) data.

The carbonate rock area within the drainage basin upstream from Bowling Green (see Figure 10) was calculated using GIS geologic map data, and the newly delineated drainage basin. The area of carbonate rock within the basin was found to be 3995.5 km^2, amounting to 94.1% of the drainage area. Of this, the overwhelming majority was the primary geologic units earlier described, including the undifferentiated Fort Payne Formation and Borden/Renfro members of the Borden Formation (Mf), the undifferentiated St. Genevieve and St. Louis Limestones, and the undifferentiated Salem, Warsaw, and Harrodsburg Limestones, amounting to 40.6%, 29.7%, and 22.1% respectively, or a total of 92.4% of the drainage area. Other carbonate formations

comprised 1.7% of the drainage area, while clastic formations, alluvium, and water comprised a combined 6% of the drainage area. Drainage basin boundaries and carbonate rock area within the upper Green River drainage basin upstream from Greensburg, Kentucky, were obtained from Osterhoudt (2014).

5.2 Barren Discharge Data

Discharge data were acquired for the period of October 1, 2012 through September 30, 2013 (Figure 14). Discharge varied greatly over the study period, with discharges ranging from 2549 to 605,980 liters per second (L/s), with an average discharge of 78,041.2 L/s. The total volume of water discharged from the Barren River for the study period was 2.46×10^{10} liters, or 2.46 km^3. Monthly total discharge (Figure 15) was greatest in May, 2013, and lowest in September, 2013. Moreover, the three lowest monthly discharge values were September 2013, October 2012, and November 2012, which is likely indicative of a relatively drier period of the hydrologic year during the local late summer through mid-fall seasons.

5.3 Water Chemistry Data

Water chemistry data including pH, temperature, and total alkalinity were obtained for the study period, with eight-hour resolution, for calculation of total DIC concentrations. Alkalinity is utilized for calculation of the total DIC concentration for each sample period, because in carbonate-dominated natural waters alkalinity can be considered proportional to the concentration of the basic carbonate species bicarbonate and carbonate (Stumm and Morgan, 1981; Drever, 1988). While the proportion of each of these species is primarily controlled by pH, where at a pH of 7 to 9 the majority of

inorganic carbon is in the form of HCO_3^-, it is necessary to include temperature and pH in the calculations in attempts to calculate the DIC concentration accurately. Temperature values (Figure 16), were reported ranging from 5.1°C to 27.3°C, with an average of 16.3°C. Water temperature follows a trend expected for the region, with a gradual fall and rise over the hydrologic year, with the local seasons. The pH values ranged from 7.05 to 8.04 (Figure 17), with an average measured pH of 7.57 pH units. The pH appears to follow a rising and falling pattern, roughly between 7.4 and 7.8 pH units, on a shorter scale than the temperature pattern, occurring multiple times throughout the year.

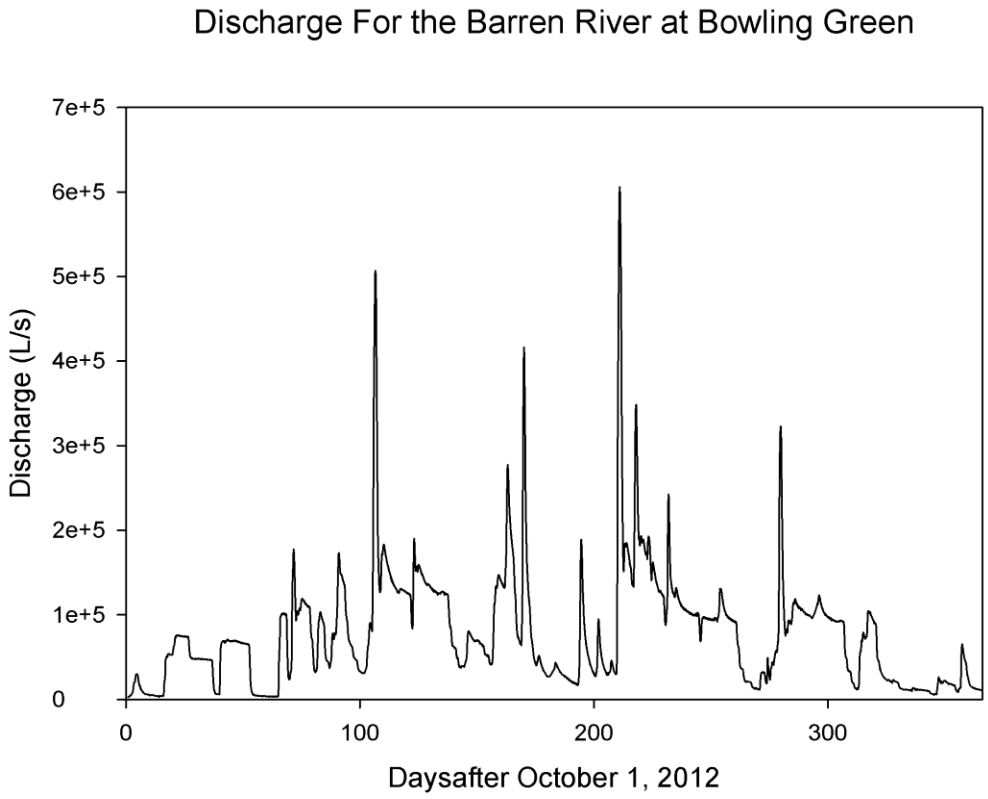

Figure 14. Discharge for the Barren River at Bowling Green. Source: BGMU (2014).

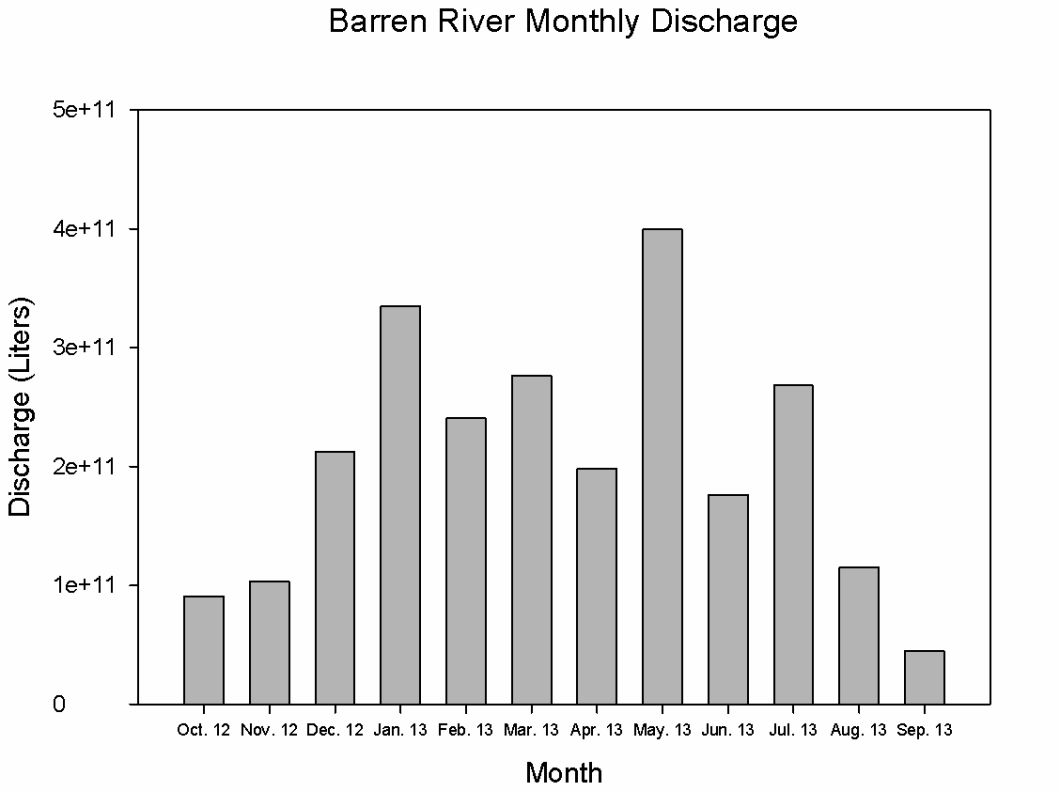

Figure 15. Barren River monthly discharge. Source: BGMU (2014).

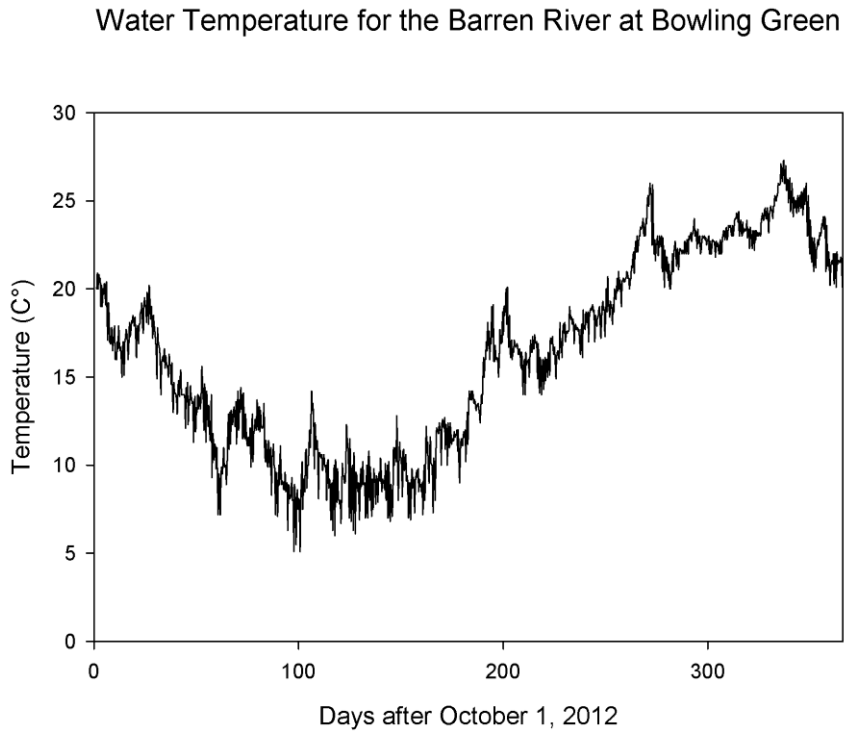

Figure 16. Water temperature for the Barren River at Bowling Green. Source: BGMU (2014).

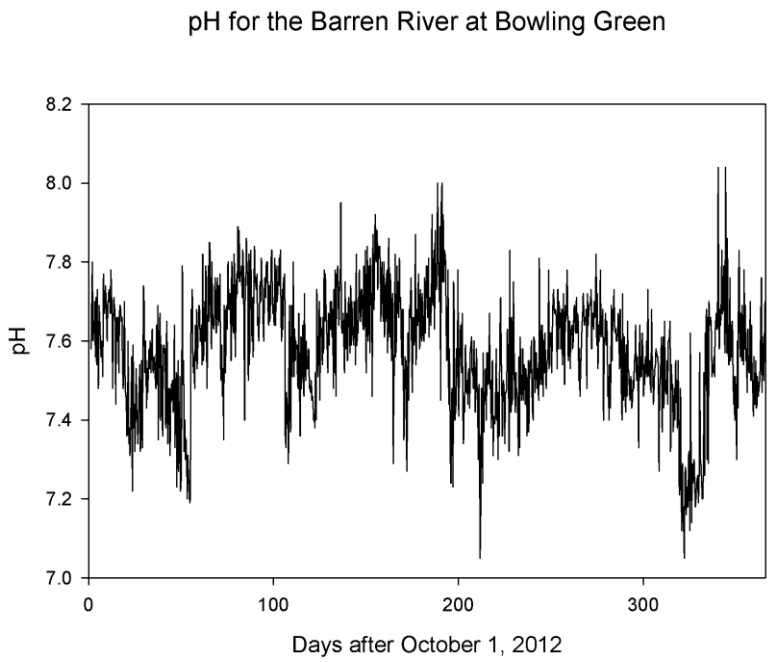

Figure 17. pH for the Barren River at Bowling Green. Source: BGMU (2014).

Alkalinity values were reported in milligrams per liter (mg/L) as $CaCO_3$ (Figure 18); alkalinity concentrations ranged from 52 to 149 mg/L, with an average on of 109.2 mg/L. When considered on a yearly scale, alkalinity exhibits a somewhat similar pattern as pH, with multiple periods of rising and falling values. The cycles exhibited by pH and alkalinity cannot be attributed to seasonal variations alone as they do not follow a similar pattern as temperature. While both of these values may be affected substantially on shorter scales by discharge, the overall trends in pH and alkalinity values on a yearly scale are primarily controlled by other influences, potentially including releases from Barren River Lake upstream. The focus of this research concerns the total annual fluxes of inorganic carbon rather than variations within the year, and so the influences on these patterns were not investigated in detail.

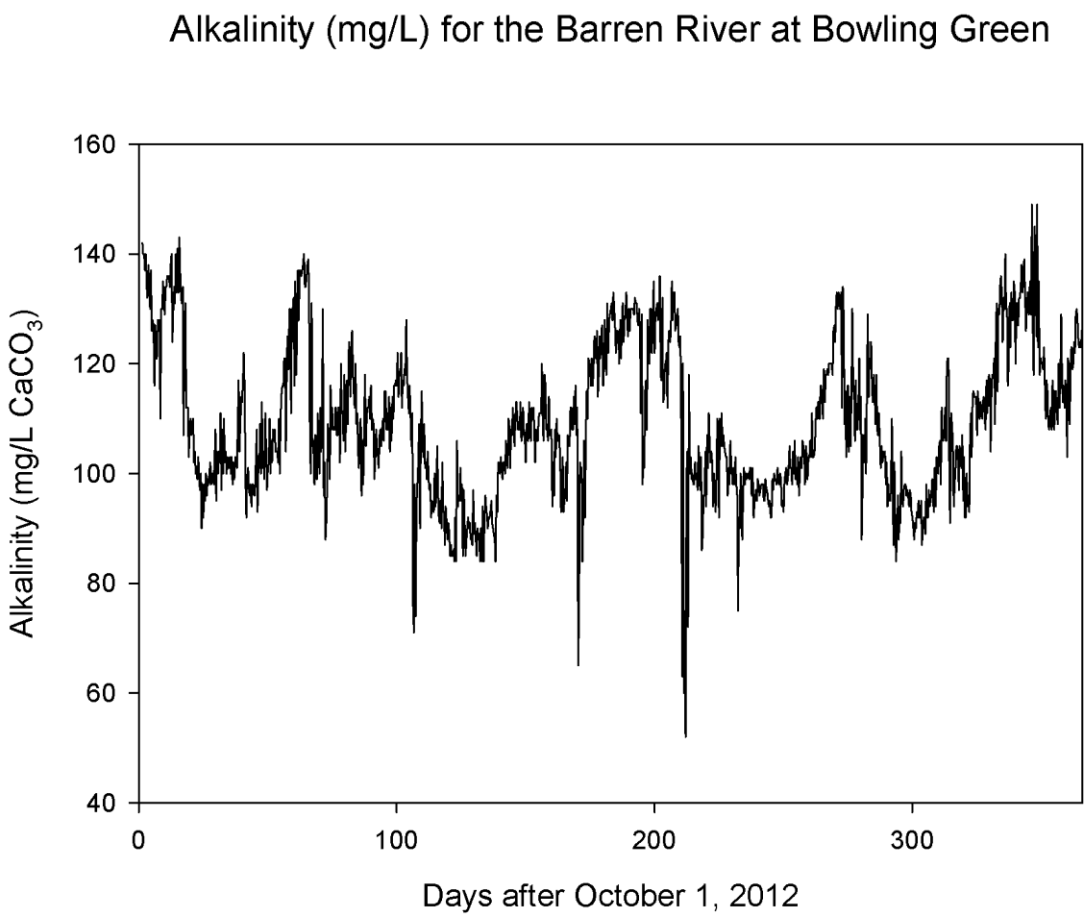

Figure 18. Alkalinity (mg/L) for the Barren River at Bowling Green. Source: BGMU (2014).

DIC values were calculated using alkalinity, temperature, and pH data. The patterns of DIC values (Figure 19) were very similar to alkalinity values, as a result of the pH range of the Barren River for the study period, with the majority of DIC in the form of bicarbonate. The average difference in alkalinity and DIC concentration was 7.55×10^{-5} mol/L of carbon, or an average difference of 3.4% resulting from the additional, relatively small mass of inorganic carbon contributed by CO_3^{2-} and $H_2CO_3^*$.

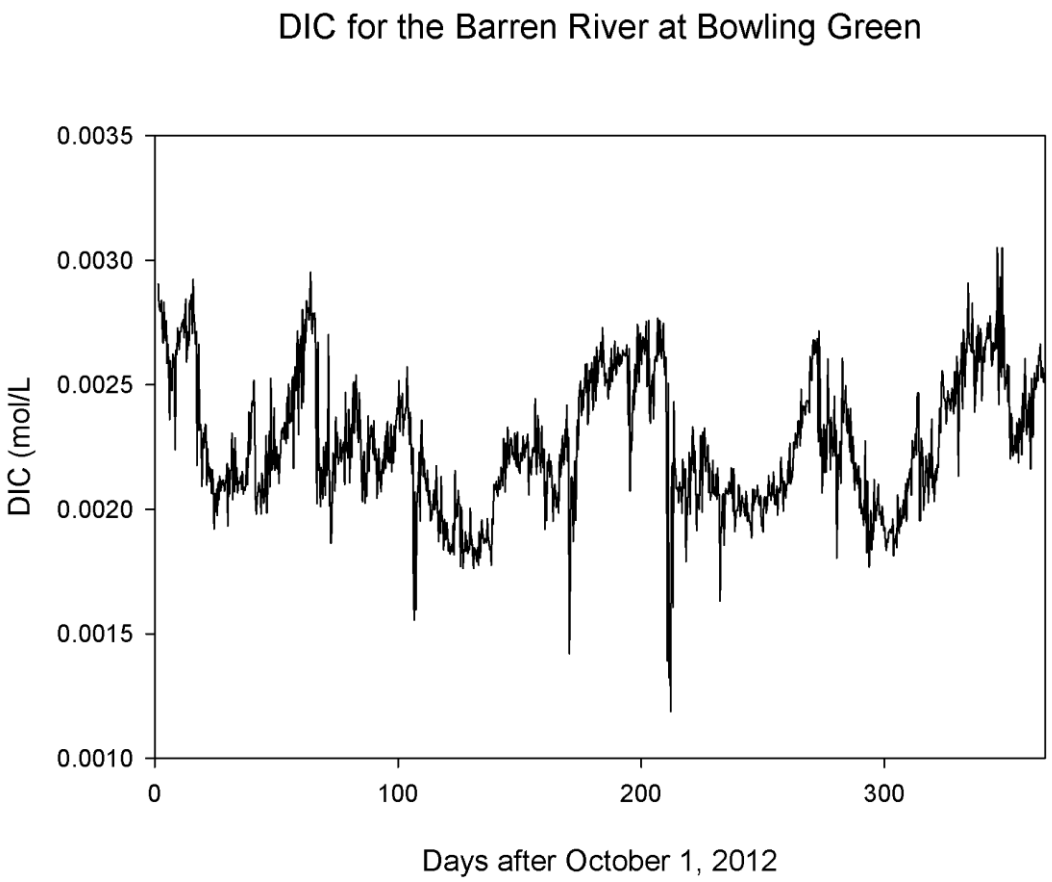

Figure 19. DIC concentration for the Barren River at Bowling Green. Source: BGMU (2014).

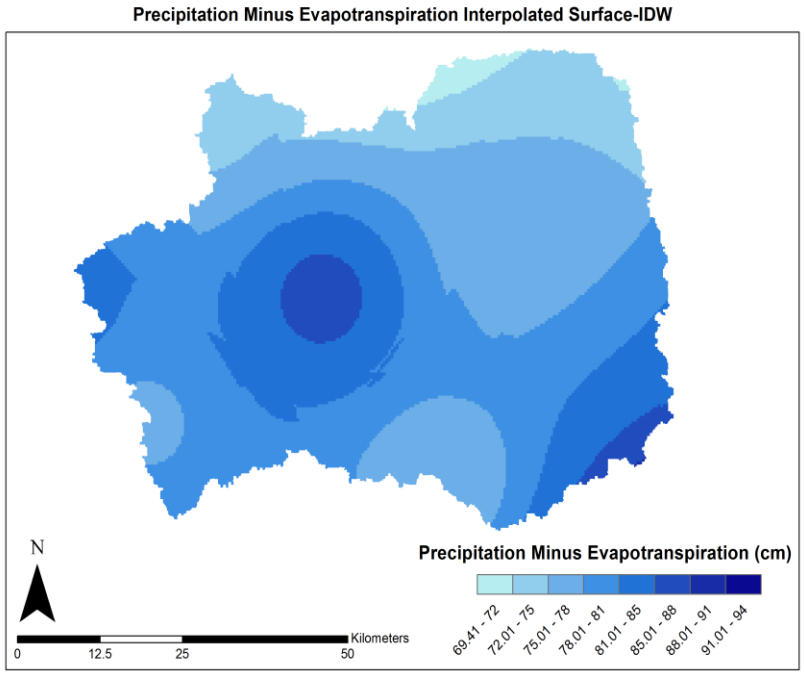

Figure 20. Precipitation minus evapotranspiration interpolated surface- IDW. Source: MRCC, 2016).

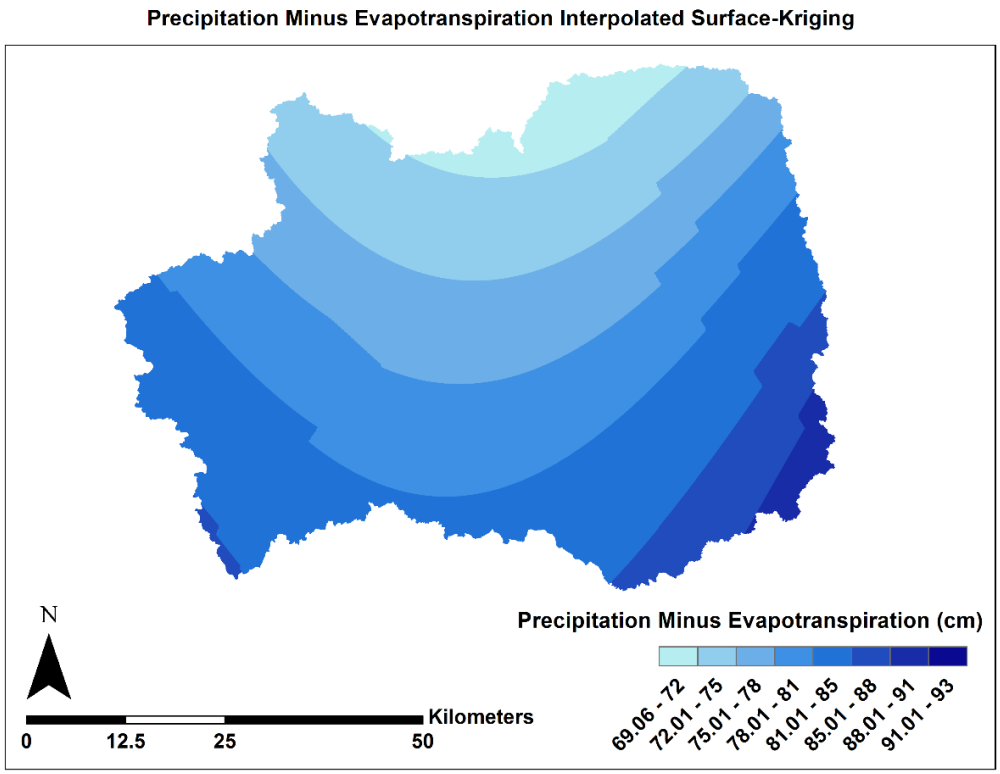

Figure 21. Precipitation minus evapotranspiration interpolated surface-Kriging. Source: MRCC, 2016).

5.4 Precipitation and Temperature Data

Precipitation and surface air temperature data for the period of study were obtained for twelve weather stations in and surrounding the drainage basin. Monthly potential evapotranspiration (PET) was estimated using the methods of Thornthwaite (1948), and used to represent the actual values of evapotraspiration (ET) over the period. These were subtracted from monthly precipitation values, and then these point P-ET data were interpolated over the drainage basin using GIS. Both Kriging and Inverse distance weighted (IDW) interpolation techniques were applied separately to the annual P-ET data (Figure 20 and 21). The resulting differences in basin-wide average values between the two methods was small, only 0.52%, with values of 79.08 and 78.67 cm for Kriging and IDW, respectively. Interpolated surface maps were generated monthly for precipitation,

potential ET, and P-ET, and basin wide average values were graphed (Figures 22 and 23) allowing for information regarding the seasonal patterns of precipitation and ET within the basin, as well as their relative effects on final P-ET. Due to the more complicated nature of the Kriging interpolation, and the greater length of time required to perform the GIS analysis using that method, and considering the close agreement between the results from the two methods, IDW was utilized for all monthly interpolation purposes, as well as later interpolation of Green River data.

Monthly precipitation (Figure 22) ranged from 3.31 cm in November, 2012, to 22.03 in July, 2013, with an average monthly precipitation of 12.06 cm, and cumulative precipitation of 144.77 cm for the year. Potential ET within the basin (Figure 23) ranged from 0.56 cm in January, 2013, to 13.98 cm in June, 2013, with an average monthly value of 6.33 cm. When considering precipitation, ET, and P-ET together (Figure 24) the seasonal effects of ET on the total available water to the flow system over a given period, or P-ET becomes clear. There is a pattern of relatively little ET in the local winter season, rising steadily through the spring, to relatively high values in the summer season. As a result of this high ET, monthly calculated values of P-ET, for June and August, 2013, were both less than 1 cm. This exhibits the much greater effect of ET on final water availability within the basin in the summer months, as expected in the region. Additionally, average basin-wide P-ET within the Green River drainage basin upstream from Greensburg, Kentucky, was determined to be 66.7cm for the hydrologic year (02/1/13-01/31/14), using IDW interpolation.

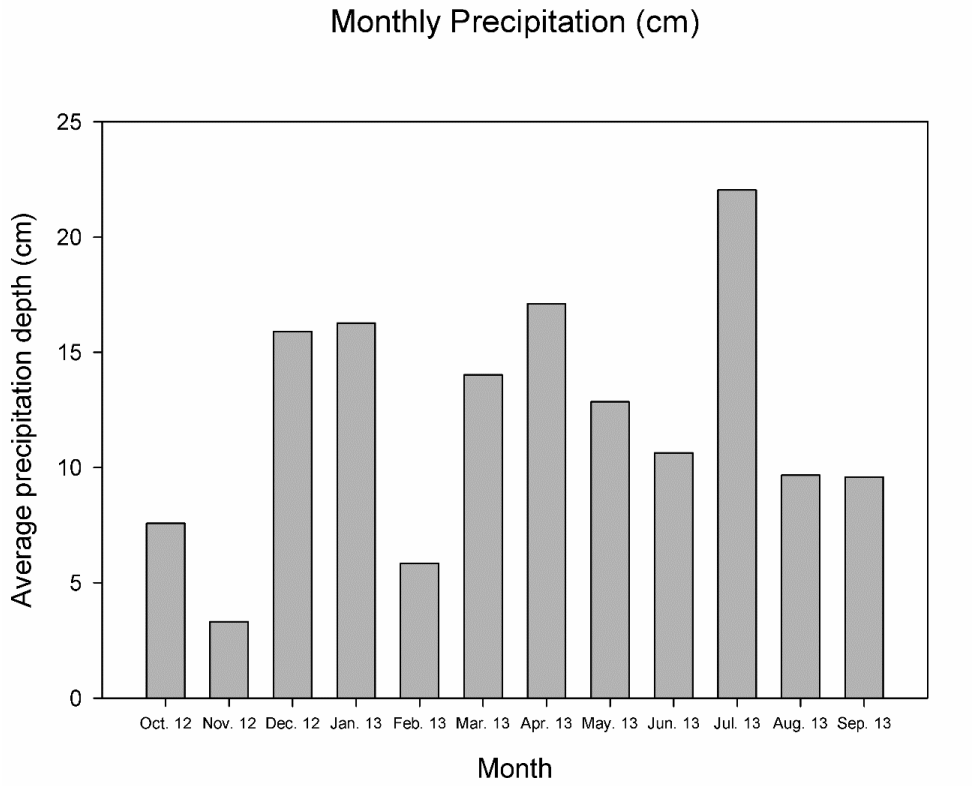

Figure 22. Monthly Precipitation (cm). Source: MWRCC (2014).

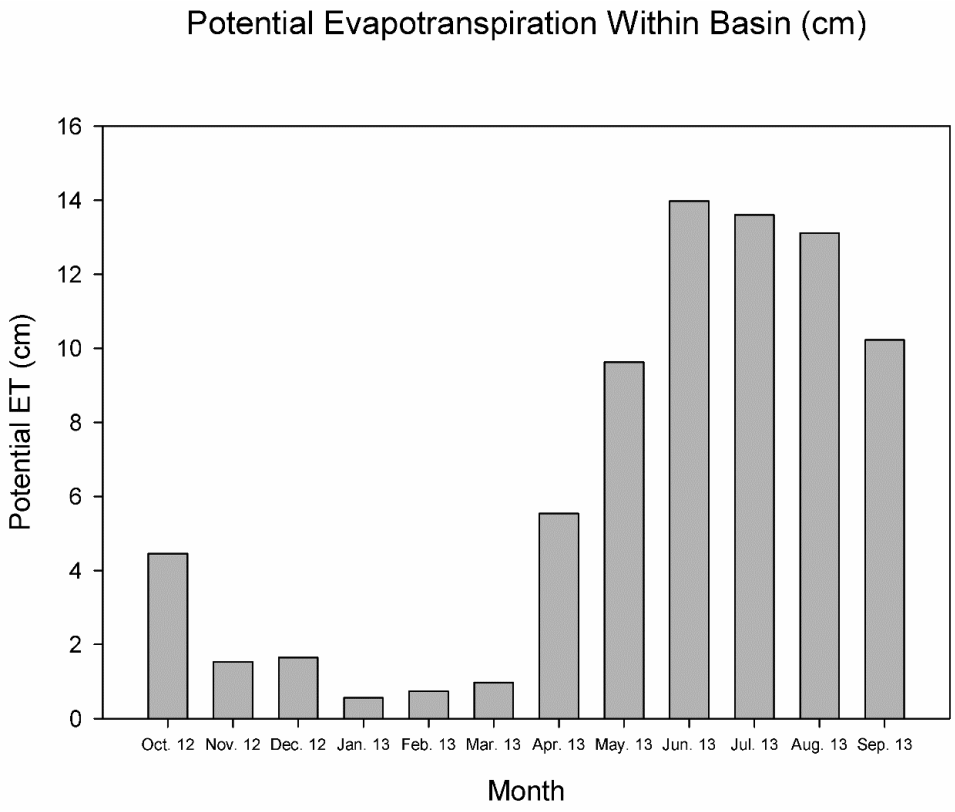

Figure 23. Potential evapotranspiration within basin (cm). Source: MWRCC (2014).

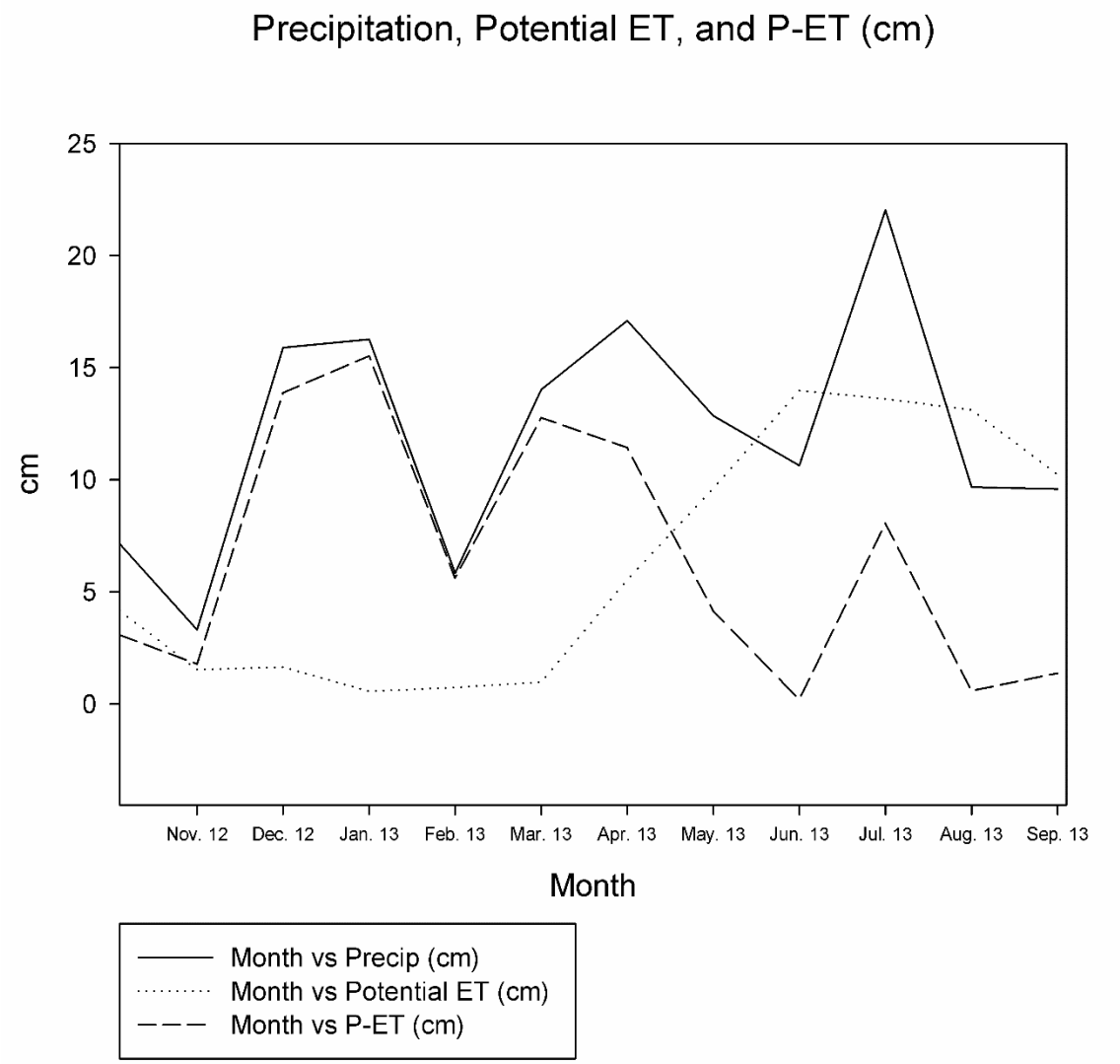

Figure 24. Precipitation, ET, and P-ET. Source: MRCC (2014).

5.5 Dissolved Inorganic Carbon Flux

The Dissolved Inorganic Carbon (DIC) flux, or total mass of inorganic carbon leaving the Barren River drainage basin for the period of study, was calculated from existing, publically available data discharge and water chemistry data. The total DIC flux for the year was found to be 6.25×10^{10} grams of carbon (Table 1). This value was then normalized following the methods of Osterhoudt (2014), by time, in days, and area of carbonate rock within the drainage basin, for comparison. The resulting normalized flux

value was $4.29x10^4$ g C day^{-1} km^{-2} (grams of carbon per day, per square kilometer of carbonate rock). This value was additionally normalized by precipitation, in order to account for the total volume of water available for carbonate rock dissolution, resulting in a value of $5.61x10^7$ g C $(km^3 H_20)^{-1}$ day^{-1} (grams of carbon per cubic kilometer of water, per day). The basins studied by Osterhoudt (2014) were two nested basins of the same river, and were not normalized by precipitation, as it was judged likely to be similar between the larger, and nested basin. As a result, comparison of normalized flux values from this work to those of Osterhoudt (2014) does not include precipitation normalization.

Basin	**Study Period**	**DIC Flux (grams of Carbon)**	**Normalized Flux (by time, area of carbonate rock)**
Barren (this study)	10/1/12-9/30/13	$6.25x10^{10}$ g	$4.29x10^4$ g C day^{-1} km^{-2}
Green-GB (this study)	2/1/13-1/31/14	$1.83x10^{10}$ g	$4.95x10^4$ g C day^{-1} km^{-2}
Green-GB (this study)	10/21/13-1/27/14	$6.65x10^9$ g	$6.75x10^4$ g C day^{-1} km^{-2}
Green-GB (Osterhoudt, 2014)	10/21/13-1/27/14	$5.58x10^9$ g	$5.66x10^4$ g C day^{-1} km^{-2}
Green-MV (Osterhoudt, 2014)	10/21/13-1/27/14	$1.96x10^{10}$ g	$5.82x10^4$ g C day^{-1} km^{-2}

Table 1. Total DIC and time-area normalized Flux values, for all data sets.

In addition to calculation of the DIC flux value of the Barren River, existing daily water chemistry and discharge data were obtained from the Greensburg water treatment plant for the basin of the Green River at Greensburg, Kentucky, in order to calculate DIC flux values for a hydrologic year, as well as for the period of study utilized by Osterhoudt (2014) for additional comparison (Table 1). The total DIC flux was calculated for a

hydrologic year, from February 1, 2013, through January 31, 2014, and found to be $1.84x10^{10}$ grams of carbon. These values were then normalized following the methods of Osterhoudt (2014), and additionally by precipitation, yielding the values 4.95g g C day^{-1} km^{-2}, and $7.43x10^{7}$ g C $(km^3 H_20)^{-1}$ day^{-1} respectively. The total DIC flux calculated for the study period by Osterhoudt (2014) (October 21, 2013- January 27, 2014) was found to be $6.65x10^{9}$ grams of carbon, with resultant normalized values of $6.74x10^{4}$ g C day^{-1} km^{-2}, and $3.37x10^{8}$ g C $(km^3 H_20)^{-1}$ day^{-1}. These DIC values were calculated and normalized in order to obtain additional flux value data points determined from existing data, to evaluate the use of existing (water treatment plant) data for these calculations, and assess the ability of the normalization techniques to capture sufficient accuracy of the flux.

5.6 Normalized Flux Comparisons

Time and area of carbonate rock normalized DIC flux values were calculated from existing data for comparison to the values obtained by Osterhoudt (2014) through the use of high resolution data loggers and are directly compared. Additionally, the values obtained in this study from existing data were further normalized by the amount of water available during each study period for dissolution (precipitation-evapotranspiration over the area of carbonate rock). This normalization results in a value of grams of carbon, per time, and per available unit of water. The use of this technique aims to account for the primary variables affecting DIC flux values, without the direct use of water chemistry, or discharge data, by establishing a relationship between total flux, and time-volume of water available. Agreement between these normalized values, and correlation between

total flux and the normalized variables would allow for estimation of DIC flux values over large areas, using only geologic and climatic data.

Time and area of carbonate rock normalized DIC flux values obtained in this study, without inclusion of precipitation minus evapotranspiration, were found to agree reasonably with those of Osterhoudt (2014), with all normalized values obtained from existing data agreeing within 26% or less. This means that other variables potentially affecting this DIC flux, and any method inaccuracy arising from shorter-than-one-year study periods used by Osterhoudt (2014), account for up to 26% error in estimation of the DIC flux when using only time and area of carbonate rock as normalization factors. Moreover, when comparing the normalized DIC flux values for the Green River drainage basin, calculated from both high resolution (Osterhoudt 2014) and existing water treatment data for the same period of study, the values were found to agree within 17%. This indicates the potential lack of precision of alkalinity measurements when using existing low-resolution data, such as daily resolution in this case. When comparing total DIC flux values, by graphing the total DIC flux versus time-area of carbonate rock, a strong positive relationship is observed (Figure 25). This relationship yields a coefficient of determination, or R^2 value, of 0.9831. The R^2 value is a measure of goodness of fit, or how well data fit a statistical model or, in this case, how well the data set fits a linear equation; for example, 0.0 indicates that there is no relationship between the data points and the line and 1.0 indicates a perfect fit. This high R^2 value without the inclusion of the precipitation minus evapotranspiration values is likely indicative of the similar hydrologic environments of the two drainage basins, located in the same climate zone and adjacent to each other. It is possible that, if this technique were applied to a much larger

area or basins in more varied climates, this relationship might well be much weaker without inclusion of precipitation minus evapotranspiration data.

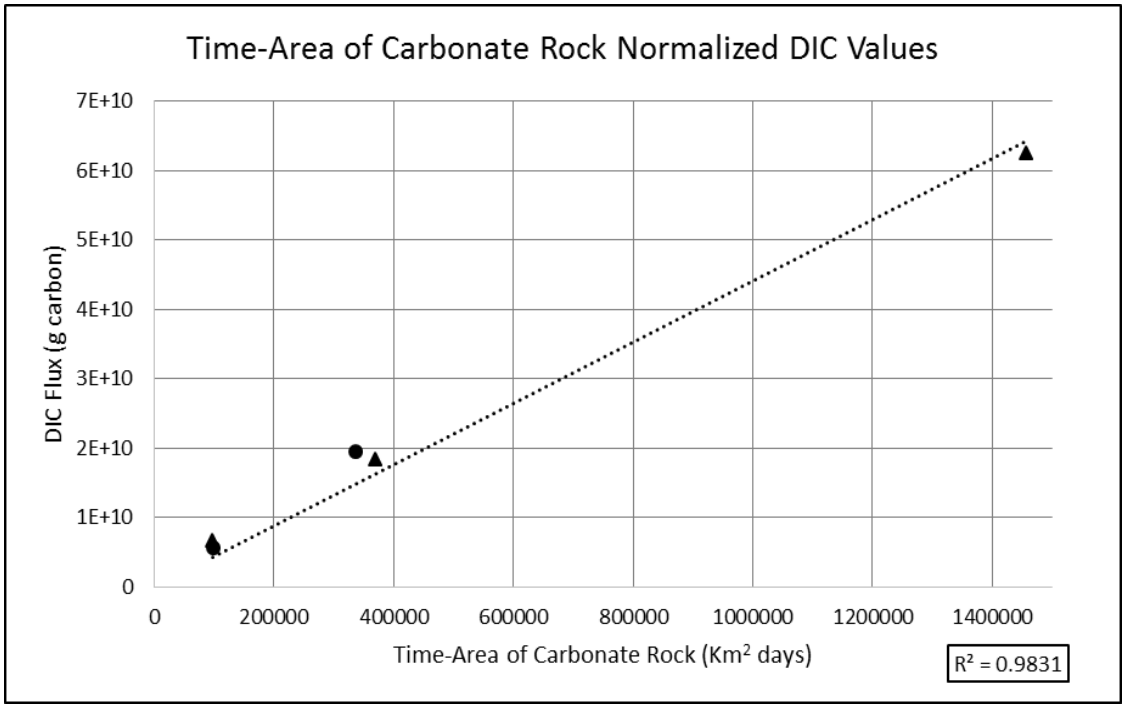

Figure 25. Time-area of carbonate rock normalized DIC values. Source: BGMU (2014), Osterhoudt, (2014).

When comparing time and volume of water normalized flux values only the Barren River hydrologic year and Green River-Greensburg hydrologic year flux values can be considered, as Osterhoudt (2014) did not account for precipitation. Using only these two data sets, only two points are available to graph, yielding no information about the linear relationship. The Barren River hydrologic year additionally was subdivided into monthly normalized flux values, generating twelve additional data points (Figure 26). When these twelve values are graphed along with the two for the Barren, and Green River hydrologic year values, the resultant R^2 value is 0.9478, which again indicates a

strong positive relationship between DIC flux and time-volume of water available for carbonate dissolution.

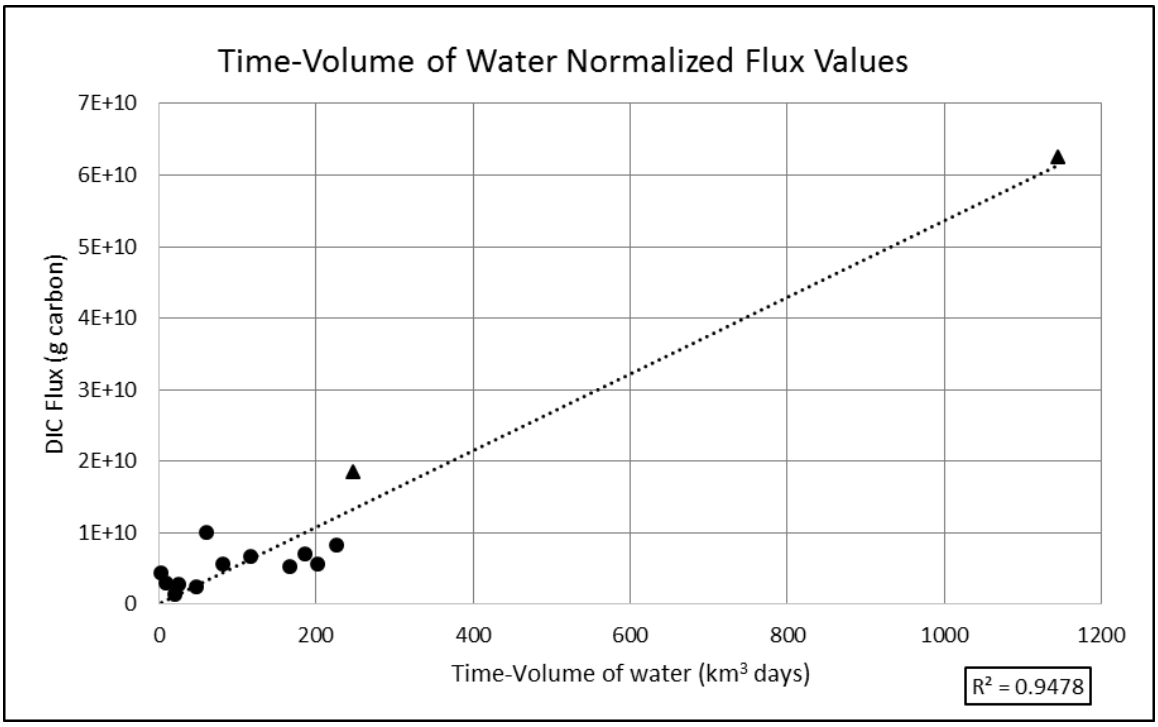

Figure 26: Time-volume of water normalized flux values. Source: BGMU (2014); Osterhoudt (2014).

5.7 Conclusions

The purposes of this study were to: 1) determine if the DIC flux from carbonate rock weathering could be accurately quantified using existing, publically available data, 2) quantify a normalized value of flux for the Barren River for a hydrologic year, and 3) determine if normalization of this flux by time in the study period and volume of water available for carbonate rock dissolution sufficiently generated values that are comparable for basins of different sizes in different climates. As part of this study, geologic and hydrologic maps were generated to determine drainage basin areas and the area of carbonate rock within the basin. Precipitation and temperature data were obtained and

used to estimate precipitation and evapotranspiration. Additionally, existing water chemistry and discharge data were obtained and utilized to calculate the DIC flux, and ultimately the time-volume of water normalized flux values. These values have been compared, and a statistical relationship between DIC flux and time-volume of water available for dissolution, has been proposed based on empirical data.

In Summary:

1. Can the inorganic carbon flux associated with carbonate mineral weathering in the Barren River basin, be quantified using existing, publically available discharge and hydrochemical data?
    - The dissolved inorganic carbon flux from carbonate mineral weathering in the Barren River basin was calculated successfully from existing, publically available data.
2. What is the volume of the inorganic carbon flux from carbonate mineral weathering for the Barren River drainage basin upstream from Bowling Green, KY, normalized by time, area of carbonate rock, and precipitation minus evapotranspiration over carbonate rock are, based on existing data?
    - The DIC flux from carbonate rock weathering within the Barren River drainage basin, normalized by time and P-ET over the area of carbonate rock, was determined to be 5.61×10^{7} g C $(km^{3} H_{2}0)^{-1}$ day^{-1} (grams of carbon per cubic kilometer of water, per day).
3. Does comparison of this normalized value with those measured by Osterhoudt (2014) suggest that this normalization process captures sufficient precision of the flux values so that this method can be expanded over large regions?

- Successful calculation of this DIC flux from existing data, and a strong positive relationship exhibited when DIC flux values are graphed against time-volume of water, suggests that this normalization process indeed captures the factors most substantially affecting this flux value in these basins.

When considering calculation of the DIC flux from carbonate rock weathering, it has been shown that existing, publically available data can be utilized with acceptable accuracy. Time-area of carbonate rock normalized DIC flux values, calculated from existing data, agree well with those of Osterhoudt (2014), with all values agreeing within 26%. Additionally, when considering the period of October 21, 2013, through January 27, 2014, for which the normalized flux was calculated using high resolution 15-minute data, and existing daily water treatment plant data, the resulting difference between the values was within 17%. This difference may be indicative of diel-scale changes to water chemistry that are masked by daily sampling. Even without the inclusion of precipitation minus evapotranspiration data, the agreement of these values show that, for the purposes of these types of study, existing data of daily or greater resolution can be utilized to calculate DIC flux.

The primary purpose of this study has been to determine if the use of a DIC flux normalization technique, involving normalization by time and volume of water available for carbonate rock dissolution, captures sufficient precision of this flux for use over larger areas. That is, if the total DIC flux for a drainage basin is dependent primarily upon time and the volume of water available for carbonate rock dissolution, and a statistical relationship can be developed between these, moving forward it should be possible to estimate this flux over large areas using this relationship with geologic and climatic data.

Multiple DIC values were calculated, the resultant normalized flux values were compared, and a linear relationship was determined between DIC flux and the product of time and volume of water available for carbonate rock dissolution. The two values obtained of 5.61×10^7 g $(km^3 H_20)^{-1}$ day^{-1}, and 7.43×10^7 g $(km^3 H_20)^{-1}$ day^{-1} agree within 25%. Moreover, a statistical relationship was determined using the two hydrologic year data sets, as well as the hydrologic year for the Barren River divided into twelve monthly normalized flux values, yielding an R^2 value of .9493. This agreement of normalized flux values, along with a strong positive relationship between DIC flux and the normalization variables, indicates that this normalization technique captures the primary signal associated with the phenomena. This indicates that the DIC flux for a drainage basin for a specific period of time may potentially be estimated using only geologic and climactic data. This could eliminate the need for the use of any data logging equipment, or the use of existing water chemistry or discharge data, in future studies attempting to quantify this flux.

The difference found between these values indicates the potential limitations of the method. The scatter associated with the monthly DIC flux values normalized by time-volume of water (Figure 25), and the slightly lower r^2 value when compared to only time-area of carbonate rock values, indicates the possibility for loss of method accuracy at smaller than yearly scales. This may be due to the potential for change in storage within the system on seasonal or monthly scales, which are generally negligible on the yearly scales. These include the use of alkalinity data to quantify bicarbonate concentrations, assuming that other sources of alkalinity-producing species are negligible within the sampled water of the existing data, as well as the use of average basin-wide precipitation

minus evapotranspiration, which is limited by: 1) the accuracy of precipitation measurement and density of measurement stations, 2) the accuracy of the potential evapotranspiration calculation, and 3) the accuracy of the interpolation of the point data into a two dimensional surface in GIS. Additionally, other factors may affect the total DIC flux within a drainage basin to varying extents, such as weathering of calcite in igneous and/or other sedimentary rocks (Amiotte Suchet et al., 2003), uptake of DIC by aquatic photosynthetic organisms (Liu et al., 2011), land-use type, and distribution within the basin, and associated soil CO_2 concentrations (Zhang, 2011), as well as other often relatively small potential fluxes.

It is impractical, however, to attempt to measure and/or quantify all the variables affecting the DIC flux in a drainage basin. Therefore, use of this method to estimate these flux values, using minimal input variables, may substantially enhance the procedure for quantifying the flux values from carbonate rock weathering over large areas. Better quantification of this flux value over large areas should allow for greater insight regarding the magnitude of the atmospheric sink of CO_2 from carbonate rock weathering over these areas and, eventually, on a global scale. More accurate quantification of this atmospheric CO_2 sink effect could clarify the role of these processes in the global carbon budget (Liu and Zhao, 2000; Liu et al., 2011; White, 2013), which could contribute to a better understanding of current climate change and potential mitigation of future climate change. Future areas of research should include further similar analysis of more rivers in order to bolster the current data set of normalized DIC flux values. This should include more rivers in diverse climatic and geologic settings in order to test the further ability of this normalization method to accurately and sufficiently capture the primary factors

affecting this carbon flux value. Additionally, more research is needed regarding the effect of aquatic vegetative uptake of DIC in rivers on the DIC flux and, thus, on the atmospheric CO_2 sink, and on the potential effects of this carbon's burial in terrestrial waterways.

References

Amiotte Suchet, P., Probst, J.-L. (1995). A global model for present-day atmospheric/soil CO_2 consumption by chemical erosion of continental rocks (GEM-CO2). *Tellus* 47B, 273–280.

Amiotte Suchet, P., Probst, J.-L., Ludwig, W. (2003). Worldwide distribution of continental rock lithology: Implications for the atmospheric/soil CO_2 uptake by continental weathering and alkalinity river transport to the oceans. *Global Biogeochemical Cycles* 17(2), 1038.

Barrenriverlake.net (2014). About Barren River Lake. Barren River Lake, KY. Online at: http://www.barrenriverlake.net/about.php (Accessed December 4, 2014).

Berner, R.A. (1989). Biogeochemical cycles of carbon and sulfur and their effect on atmospheric oxygen through phanerozoic time. *Paleogeography, Paleoclimatology, Paleoecology* 75, 97–122.

Berner, R. A., Lasaga, A. C., Garrels, R. M. (1983). The carbonate-silicate geochemical cycle and its effect on atmospheric carbon dioxide over the past 100 million years. *American Journal of Science* 283, 641–683.

BGMU (Bowling Green Municipal Utilities) (2014). *Statistics*. Bowling Green, KY: BGMU, Water Treatment Plant. Online at www.bgmu.com.

Cao, J., Yang, H., Kang, Z. (2011). Preliminary regional estimation of carbon sink flux by carbonate rock corrosion: A case study of the Pearl River Basin. *Chinese Science Bulletin* 56(35), 3766–3773.

Cao, J., Yuan, D., Groves, C., Huang, F., Yang, H., Lu, Q. (2012). Carbon fluxes and sinks: the consumption of atmospheric and soil CO_2 by carbonate rock dissolution. *Acta Geologica Sinica* 86(4), 963–972.

Cole, J.J., Prairie, Y.T., Caraco, N.F., McDowell, W.H., Tranvik, L.J., Striegl, R.G., Duarte, C.M., Kortelainen, P., Downing, J.A., Middleburg, J.J., Melack, J. (2007). Plumbing the Global Carbon Cycle: Integrating Inland Waters into the Terrestrial Carbon Budget. *Ecosystems* 10(1), 172–185.

Cox, P.M., Betts, R.A., Jones, C.D., Spall, S.A. (2000). Acceleration of global warming due to carbon-cycle feedbacks in a coupled climate model. *Nature* 408(9), 184–187.

Drever, J.I. (1988). *The Geochemistry of Natural Waters.* New York: Prentice Hall.

Drever, J.L. (1997). *The Geochemistry of Natural Waters: Surface and Groundwater Environments*. New York: Prentice Hall.

Dreybrodt, W. (1988). *Processes in Karst Systems: Physics, Chemistry, and Geology*. Heidelberg, Germany: Springer.

Dürr, H.H., Meybeck, M., Dürr, S.H. (2005). Lithologic composition of the Earth's continental surfaces derived from a new digital map emphasizing riverine material transfer. *Global Biogeochemical Cycles* 19(4), GB4S10.

Einsele, G., Yan, J., Hinderer, M. (2001). Atmospheric carbon burial in modern lake basins and its significance for the global carbon budget. *Global and Planetary Change* 30(3), 167–195.

Falkowski, P., Scholes, R.J., Boyle, E., Canadell, J., Canfield, D., Elser, J., Gruber, N., Hibbard, K., Hogberg, P., Linder, S., Mackenzie, F.T., Moore III, B., Pederson, T., Rosenthal, Y., Seitzinger, S., Smetacek, V., Steffen, W. (2000). The Global Carbon Cycle : A Test of Our Knowledge of Earth as a System. *Science* 290(5490), 291–296.

Fan, S., Gloor, M., Mahlman, J., Pacala, S., Sarmiento, J., Takahashi, T., Tans, P.P. (1998). A Large Terrestrial Carbon Sink in North America Implied by Atmospheric and Oceanic Carbon Dioxide Data and Models. *Science* 282, 442–446.

Gibbs, M.T., Kump, L.R. (1994). Global chemical erosion dusing the last glacial maximum and the present: sensitivity to changes in lithology and hydrology. *Paleoceonography* 9(4), 529–543.

Gott, J. (2014). Personal communication on 23 November, 2014.

Grabowski, G.J., (2001). Contributions to the geology of Kentucky-Mississippian system. Alexandria, VA: United States Geological Survey. Online at: http://pubs.usgs.gov/pp/p1151h/miss.html (Accessed November 30, 2014).

Groves, C., Meiman, J. (2001). Inorganic carbon flux and aquifer evolution in the south central Kentucky karst. In Kuniansky, E.L. (ed.). St. Petersburg, FL: *US Geological Survey Karst Interest Group Proceedings, Water-Resources Investigations Report 01-4011*, pp. 99–105.

Groves, C., Meiman, J. (2002). *Strong acids and the carbonate mineral weathering atmospheric sink*. Paper presented at the Geological Society of America Conference, Denver, CO, October 27. Available online at: https://gsa.confex.com/gsa/2002AM/finalprogram/abstract_41887.htm

Groves, C., Meiman, J. (2005). Weathering, geomorphic work, and karst landscape evolution in the Cave City groundwater basin, Mammoth Cave, Kentucky. *Geomorphology* 67(1-2), 115–126.

Groves, C., Cao, J., Cheng, Z. (2012). Response-Carbon shifted but not sequestered. *Science 335*(6069), 655.

Groves, C., Meiman, J., Despain, J., Liu, Z., Yuan, D. (2002). Karst Aquifers as Atmospheric Carbon Sinks: An Evolving Global Network of Research Sites. In Kuniansky, E.L. (ed.). *U.S. Geological Survey Water-Resources Investigations Report 02-4174*, Shepherdstown, WV, pp. 32–39.

Hach (2012). *PH USEPA Electrode Method, Method 8156*. Loveland, CO: Hach Company. Online at: http://www.hach.com/asset-get.download-en.jsa?code=56935 (Accessed November 16, 2014).

Harned, H.S., Owen, B.B., and King, C.V. (1959). The physical chemistry of electrolytic solutions. *Journal of the Electrochemical Society* 106(1), 15C-15C.

Hartmann, J., Jansen, N., Dürr, H.H., Kempe, S., Köhler, P. (2009). Global CO_2-consumption by chemical weathering : what is the contribution of highly active weathering regions? *Global and Planetary Change* 69(4), 185–194.

Haryono, E. (2011). *Atmospheric carbon dioxide sequestration trough karst denudation processes preliminary estimation from Gunung Sewu karst*. In Proceedings of the Asian Trans-Disciplinary Karst Conference, November 17-19, Bogor, Indonesia, pp. 203–207.

He, S.-Y., Kang, Z.-Q., Li, Q.-Y., Wang, L.-L. (2013). The Utilization of Real-Time High Resolution Monitoring Techniques in Karst Carbon Sequestration: A Case Study of the Station in Banzhai Subterranean Stream Catchment. *Advances in Climate Change Research* 3(1), 54–58.

Hoffert, M.I., Caldeira, K., Jain, A.K., Haites, E.F., Harvey, L.D., Potter, S.D., Schlesinger, M.E., Schneider, S.H., Watts, R.G., Wigley, T.M., Wuebbles, D.J. (1998). Energy implications of future stabilization of atmospheric CO2 content. *Nature* 395, 881–884.

Jiang, Z., Yuan, D. (1999). CO 2 source-sink in karst processes in karst areas of China. *Episodes* 22(1), 33–35.

KGS (Kentucky Geological Survey) (2012). *The Mississippian Plateau or Pennyroyal Region*. Lexington KY: KGS, University of Kentucky. Online at: http://www.uky.edu/KGS/geoky/regionPennyroyal.html (Accessed November 23, 2014).

KGS (Kentucky Geological Survey) (2014). *Geospatial Data Library*. Lexington, KY: KGS, University of Kentucky. Online at: http://www.uky.edu/KGS/gis/kgs_gis.htm (Accessed 16 November, 2014).

KY Mesonet (2016) *Yearly Summaries*. Bowling Green, KY: Western Kentucky University, Kentucky Mesonet. Online at: http://www.kymesonet.org/summaries.html (Accessed January 12, 2016)

Liu, Z., Dreybrodt, W. (1997). Dissolution kinetics of calcium carbonate minerals in H_20-CO_2 solutions in turbulent flow : The role of the diffusion boundary layer and the slow reaction $H_20 + CO_2 <> H + HCO_3$. *Geochemica et Cosmochimica Acta* 61(14), 2879–2889.

Liu, Z., Zhao, J. (2000). Contribution of carbonate rock weathering to the atmospheric CO_2 sink. *Environmental Geology* 39(9), 1053–1058.

Liu, Z., Dreybrodt, W., Liu, H. (2011). Atmospheric CO_2 sink: Silicate weathering or carbonate weathering? *Applied Geochemistry* 26, S292–S294.

Liu, Z., Dreybrodt, W., Wang, H. (2008). A possible important CO_2 sink by the global water cycle. *Chinese Science Bulletin* 53(3), 402–407.

Liu, Z., Dreybrodt, W., Wang, H. (2010). A new direction in effective accounting for the atmospheric CO_2 budget: Considering the combined action of carbonate dissolution, the global water cycle and photosynthetic uptake of DIC by aquatic organisms. *Earth-Science Reviews* 99(3-4), 162–172.

Ludwig, W., Amiotte-Suchet, P., Probst, J.L. (1999). Enhanced chemical weathering of rocks during the last glacial maximum: a sink for atmospheric CO_2? *Chemical Geology* 159(1-4), 147–161.

Ludwig, W., Amiotte-Suchet, P., Munhoven, G., Probst, J.L. (1998). Atmospheric CO_2 consumption by continental erosion: present-day controls and implications for the last glacial maximum. *Global and Planetary Change* 16, 107–120.

Lüthi, D., Le Floch, M., Bereiter, B., Blunier, T., Barnola, J.-M., Siegenthaler, U., Raynaud, D., Jouzel, J., Fischer, H., Kawamura, K., Stocker, T.F. (2008). High-resolution carbon dioxide concentration record 650,000-800,000 years before present. *Nature* 453(7193), 379–82.

McClanahan, K.N. (2014). *Carbon Cycling Dynamics Inferred from Carbon Isotope Sourcing in a Mid-Latitude Karst-Influenced River*. Master's Thesis in Geoscience, Department of Geography and Geology, Western Kentucky University. Online at: http://digitalcommons.wku.edu/theses/1393/

McDowell, R.C. (2001). *Contributions to the geology of Kentucky-Structural Geology*. Alexandria, VA: United States Geological Survey. Online at: http://pubs.usgs.gov/pp/p1151h/structure.html (Accessed November 30, 2014).

Meiman, J., (2006). *Mammoth Cave National Park Water Resources Management Plan*. Washington, DC: United States Department of the Interior, National Park Service.

Meybeck, M. (1987). Global chemical weathering of surficial rocks estimated from river dissolved loads. *American Journal of Science* 287, 401–428.

Milankovitch, M. (1941). *Canon of Insolation and the Ice Age Problem*. Belgrade: Koniglich Serbische Akademie.

MRCC (Midwestern Regional Climate Center) (2016) *Cli-MATE Online Data Portal.* Champaign, IL: MRCC. Online at: http://mrcc.isws.illinois.edu/CLIMATE/ (Accessed January 12, 2016).

Newell, W.L. (2001). *Contributions to the geology of Kentucky-Physiography.* Alexandria VA: United States Geological Survey. Online at: http://pubs.usgs.gov/pp/p1151h/physiography.html (Accessed November 30, 2014).

Osterhoudt, L.L. (2014). *Impacts of Carbonate Mineral Weathering on Hydrochemistry of the Upper Green River Basin, Kentucky*. Master's Thesis in Geoscience, Department of Geography and Geology, Western Kentucky University, Bowling Green, KY. Online at: http://digitalcommons.wku.edu/theses/1337/

Palmer, A.N. (1981). *A Geological Guide to Mammoth Cave National Park.* Teaneck, NJ: Zephephyrus Press.

Palmer, A.N., Palmer, M.V. (eds.), (2009). *Caves and Karst of the USA*. Huntsville, AL: National Speleological Society.

Peel, M.C., Finlayson B.L., McMahon T.A. (2007). Updated world map of the Köppen-Geiger climate classification. *Hydrology and Earth System Sciences Discussions* 4: 439-473.

Plummer, L.N., Wigley, T.M., Parkhurst, D.L. (1978). The kinetics of calcite dissolution in CO_2-water systems at 5 to 60 degrees C and 0.0 to 1.0 atm CO_2. *American Journal of Science* 278, 179–216.

Raymond, P.A., Caraco, N.F., Cole, J.J., Ab, B. (1997). Carbon Dioxide Concentration and Atmospheric Flux in the Hudson River. *Estuaries* 20(2), 381–390.

Sarmiento, J., Sundquist, E.T. (1992). Revised budget for the oceanic uptake of anthropogenic carbon dioxide. *Nature* 356, 589–593.

Sauer, C.O., Leighly, J., McMurry, K.C., Newman, C.W., Burroughs, W.G. (1927). *Geography of the Pennyroyal: a study of the influence of geology and physiography upon industry, commerce and life of the people.* Lexington, KY: Kentucky Geological Survey.

SDSU (San Diego State University) (2016). *Online hydraulic and hydrologic calculations.* San Diego, CA: SDSU. Online at: http://onlinecalc.sdsu.edu/ (Accessed January 12, 2016).

Shackleton, N.J. (2000). The 100,000-Year Ice-Age Cycle Identified and Found to Lag Temperature, Carbon Dioxide, and Orbital Eccentricity. *Science* 289, 1897–1902.

Siegenthaler, U., Sarmiento, J. (1993). Atmospheric carbon dioxide and the ocean. *Nature* 365(6442), 119–125.

Sigman, D.M., Boyle, E.A. (2000). Glacial/interglacial variations in atmospheric carbon dioxide. *Nature* 407, 859–869.

SM (Standard Methods) (2006a). *2550 Temperature.* Washington, DC: American Public Health Association, American Water Works Association, Water Environment Foundation. Online at: http://www.standardmethods.org/store/ProductView.cfm?ProductID=64 (Accessed November 16, 2014).

SM (Standard Methods) (2006b). *2320 Alkalinity.* Washington, DC: American Public Health Association, American Water Works Association, Water Environment Foundation. Online at: http://www.standardmethods.org/store/ProductView.cfm?ProductID=56 (Accessed November 16, 2014).

Stumm, M., Morgan, J.J. (1981). *Aquatic Chemistry: An Introduction Emphasizing Chemical Equalibria in Natural Waters*. New York, NY: John Wiley and Sons.

Sundquist, E.T. (1993). The global carbon dioxide budget. *Science* 259(5097), 934–941.

Sweeting, M. (1972). *Karst Landforms*. London, UK: Macmillan Press.

Tans, P.P., Keeling, R. (2014). *Trends in Atmospheric Carbon Dioxide*. Silver Springs, MD: NOAA/ESRL (National Oceanic & Atmospheric Administration/Earth System Research Laboratory), Scripps Institution of Oceanography: Online at: *http://www.esrl.noaa.gov/gmd/ccgg/trends/* (Accessed October 27, 2014).

Tans, P.P., Fung, I.Y., Takahashi, T. (1990). Observational contrains on the global atmospheric CO_2 budget. *Science* 247(1431), 31–38.

Ternon, J., Oudot, C., Dessier, A., Diverres, D. (2000). A seasonal tropical sink for atmospheric CO_2 in the Atlantic ocean: the role of the Amazon River discharge. *Marine Chemistry* 68(3), 183–201.

Thornthwaite, C.W. (1948). An approach toward a rational classification of climate. *Geographical Review* 38(1), 55-94.

USDA (United States Department of Agriculture) (2014). *Natural Resource Conservation Service Geospatial Data Gateway*. Washington DC: USDA. Online at: http://datagateway.nrcs.usda.gov/GDGHome.aspx (Accessed November 16, 2014).

USGS (United States Geological Survey) (2014a). *USGS 03314500 Barren River at Bowling Green, KY*. Alexandria, VA: USGS, National Water Information System: Web Interface. Online at: http://waterdata.usgs.gov/nwis/inventory/?site_no=03314500&agency_cd=USGS (Accessed November 23, 2014).

USGS (United States Geological Survey) (2014b). *National Hydrography Dataset*. Alexandria, VA: USGS, Hydrography. Online at: http://nhd.usgs.gov/ (Accessed 11/30/14).

USGS (United States Geological Survey) (2016*). USGS 03306500 Green River at Greensburg, KY*. Alexandria, VA: USGS, National Water Information System: Web Interface. Online at: http://waterdata.usgs.gov/ky/nwis/uv?site_no=03306500 (Accessed 12 January, 2016).

White, W.B. (2013). Carbon fluxes in Karst aquifers: Sources, sinks, and the effect of storm flow. *Acta Carsologica* 42(2-3), 177–186.

Yang, H., Xing, Y., Xie, P., Ni, L., Rong, K. (2008). Carbon source/sink function of a subtropical, eutrophic lake determined from an overall mass balance and a gas exchange and carbon burial balance. *Environmental Pollution* 151(3), 559–68.

Yuan, D. (1997). The carbon cycle in karst. *Zeitschrift Fur Geomorphologie* 108, 91–102.

Zhai, W., Dai, M., Guo, X. (2007). Carbonate system and CO_2 degassing fluxes in the inner estuary of Changjiang (Yangtze) River, China. *Marine Chemistry* 107(3), 342–356.

Zhang, C. (2011). Carbonate rock dissolution rates in different landuses and their carbon sink effect. *Chinese Science Bulletin 56*(35), 3759–3765.

Zhang, C., Yuan, D., Cao, J. (2005). Analysis of the environmental sensitivities of a typical dynamic epikarst system at the Nongla monitoring site, Guangxi, China. *Environmental Geology 47*(5), 615–619.